Master's Degree in Astrophysics

2022-2024

High-resolution cross-correlation transmission spectroscopy with GIANO-B

Pedro Pablo Meni Gallardo

Supervisor: Hannu Parviainen

San Cristóbal de La Laguna, 2024

Resumen

Desde que los primeros exoplanetas fueron descubiertos, hemos intentado llegar cada vez más lejos. Los primeros planetas descubiertos fueron los Júpiters calientes, planetas del tamaño del orden de Júpiters que tienen un periodo de rotación más cortos que Mercurio. Estos nos ayudaron a aclarar modelos de formación de sistemas planetarios y a entender el funcionamiento de las atmósferas de los gigantes gaseosos.

Debido a los procesos de formación de estos planetas y a su cercanía a sus estrellas centrales, lo que se espera de sus atmósferas es que estén dominadas por metales y que todas las moléculas complejas que pudieran formarlas estén disociadas debido a las altas temperaturas. Normalmente, el estudio y análisis de estos planetas giran alrededor de buscar elementos como helio, hierro, carbono, magnesio, etc. Debido que estas especies dominan en opacidad en el rango del óptico.

Cuando se comprendieron mejor estas atmósferas, empezaros a realizarse estudios de baja resolución en los que se buscaba ver el efecto que sufría la luz de las estrellas anfitrionas al ser filtrada por los Júpiters calientes durante los tránsitos. Debido a que eran métodos de baja resolución los estudios se limitaban a los metales mencionados con anterioridad, principalmente, helio.

En los últimos años, se han implementado procesos de alta resolución para comprobar la existencia de moléculas complejas u otros metales en este tipo de atmósferas. En mi caso, apliqué "cross-correlation", método presentado por primera vez en Snellen et al. [2010] y que se basa en el método de correlación cruzada que es una medida de la similitud entre dos señales, frecuentemente usada para encontrar características relevantes.

Mis dos principales objetivos son adaptar el código empleado por la Dra. M. Stangret en Stangret et al. [2020, 2021, 2022], para datos del HARPS-N a observaciones de GIANO-B y aplicar dicho código a planetas que aún no han sido analizados en este rango espectral, en busca de moléculas complejas características del rango infrarrojo cercano como agua, metano, monóxido de carbono, dióxido de carbono, hidruro de hierro y ácido cianhídrico.

Mis datos fueron obtenidos de observaciones realizadas mediante "nodding" con la configuración ABAB. A partir de estas, mis colaboradores del INAF, Mario Basilicatta y Paolo Giacobbe, usando GOFIO y GUIbrush, han calibrado los datos en longitud de onda; han obtenido gráficas de la evolución de la señal-ruido y del desviamiento de cada orden en base al "nodding"; han alineado los espectros; y han calculado los principales parámetros necesarios para la aplicación de la "cross-correlation", tales como la semi-amplitud de velocidad, $\mathrm{K_p}$, radio del planeta, velocidad sistemática, etc.

Tras esto, me he encargado de seleccionar los órdenes útiles para cada espectro, dejando fuera aquellos que habían sufrido un gran desplazamiento durante el "nodding" y los que estaban completamente saturados por la absorción telúrica; enmascarar los píxeles problemáticos, los píxeles caliente, valores que se desvían más de 5σ y los fríos, pixeles que toman valores negativos debido al procedimiento por el cual mis colaboradores han extraído los "flats"; y normalizar los espectros, usando un método que se basa en dividir cada orden de cada espectro en 50 trozos y de cada trozo seleccionar los 50 valores más altos para crear un polinomio que se ajuste a esos valores, de forma que al dividir el espectro de cada orden por ese polinomio, este quede perfectamente normalizado.

Una vez nuestros espectros estaban propiamente reducidos, he aplicado el método SYSREM, un

método de tipo ACP que compara la varianza de los valores de una matriz de forma que elimina las señales correlacionadas de múltiples series de tiempo, es decir, se encarga de eliminar los errores sistemáticos de nuestros datos. Cabe destacar que, para mi, la contaminación telúrica y la señal de la estrella serán errores sistemáticos, además de los inducidos por la instrumentación y la electrónica. Esto es debido a que estas señales se mantienen en el tiempo y son una constante a lo largo de todos los datos, siendo una suerte de "errores" que me impiden ver la señal proveniente del planeta. Es necesario aplicar varias iteraciones de este método, ya que es un método escalado, es decir, en la primera interacción elimina errores relacionados con la masa de aire, en la segunda con la extinción, y así hasta que desecha la señal de la estrella dejando la del planeta completamente libre. Yo he realizado 15 iteraciones, simplemente para alcanzar la señal-ruido óptima, aunque normalmente, con 8/9 iteraciones es suficiente.

A pesar de tener el espectro planetario, necesitaba unos modelos atmosféricos, en mi caso los he desarrollado usando petitRADTRANS, Mollière et al. [2019]. Dado que trabajaba con Júpiters calientes y ultra calientes, la obtención de estos modelos fue muy simple ya que pude ignorar efectos como el Rayleigh o el continuo de gas, debido a las condiciones de mis planetas. Solo necesité especificar el vector de presiones, los parámetros físicos del planeta como el radio, el semieje mayor, la temperatura de equilibrio, la gravedad superficial, etc. En mi caso, he seleccionado las moléculas ya mencionadas y he desarrollado atmósferas de un único elemento.

Una vez tenía los datos del planeta y los modelos, pude aplicar la "cross-correlation". Primero necesité interpolar los modelos con nuestros datos, ya que los modelos producidos tienen una resolución de ~ 1000000 y no están divididos en órdenes, mientras que mis datos tienen una resolución de ~ 50000. Cuando mis datos y los modelos cuadraron, cree un vector de velocidad radial desde -225 km/s hasta 225 km/s en pasos de 2.7 km/s para introducirlo en la función CrosscorrRV del paquete pyAstronomy y poder realizar el análisis en el marco de la velocidad radial. Tras esto, apliqué la "cross-correlation" entre cada orden de los espectros reducidos por SYSREM y los órdenes del modelo, obteniendo como resultado un mapa de residuos para cada orden. Uní esos mapas en uno solo, para poder ver la evolución temporal, a lo largo de la observación, de la señal del planeta en un mapa de residuos único. Otros resultados que obtuve fueron los mapas de $\mathrm{K_p}$ y la CCF, que es una "rodaja" en 2D del mapa de $\mathrm{K_p}$ para los parámetros del planeta.

Los sistemas que he seleccionado son HAT-P-57 b, KELT-17 b, KELT-21 b, WASP-189 b, para continuar con el estudio previamente realizado en Stangret et al. [2021], y HD 189733 b, para mostrar las flaquezas que tiene nuestro análisis en el caso de planetas un poco mas complejos.

En este trabajo, he hecho una detección clara, en el caso de KELT-17 b para la noche del 26-01-2019, hay una detección de 4.8σ de FeH, esta detección es muy clara y nunca había sido detectada. También hay otros caso como una detección de agua en HAT-P-57 b, en la noche del 28-06-2019, con una significancia de 3.6σ o una de dióxido de carbono con 4.7σ, en la noche del y 23-06-2019, que no he valorado como detecciones completamente debido a la alta incertidumbre de su $\mathrm{K_p}$ y a pérdidas de señal que se sufrieron durante la observación. Para el resto de planetas o noches, no ha habido ninguna detección.

En general ha sido un trabajo muy satisfactorio y nutritivo en el que no solo he aprendido a

desarrollar una pipeline capaz de realizar este tipo de análisis y a analizar estos resultados. Si no que también he hecho descubrimientos para nada desdeñables que podrían ayudar a futuros estudios de este tipo de planetas.

Abstract

Since the first exoplanet was found, we have tried to discover everything about them. In this work, we have centred on studying hot and ultra-hot Jupiters atmosphere.

Due to the way they are formed, the main composition of these planets is related to the stellar atmosphere composition like helium, iron, magnesium, carbon, etc. Mostly metals that dominate the opacity in the optical range where the main studies have been done. In my case, I am analyzing spectra form NIR from GIANO-B, looking for complex molecules, H_2O, CO, CO_2, CH_4, HCN and FeH, using high-resolution transmission espectroscopy.

The two main goals of this work are to adapt a high-resolution cross-correlation spectroscopy analysis pipeline developed for optical HARPS-N spectroscopy by Dr. M. Stangret to be used with GIANO-B spectroscopy observed in NIR; and to apply the pipeline to previously unstudied GIANO-B transmission spectroscopy observations in order to search for signatures of molecules in hot Jupiter atmospheres.

For achieving these goals, I have developed my pipeline basing on Dr. M. Stangret's previous work and improving it for my wavelength range of study. I received my data calibrated in wavelength and with all the important parameters already calculated from my collaborators, Mario Basilicatta and Paolo Giacobbe. After this, I selected the useful orders basing on the information they sent me and the absorption bands from our atmosphere. Once the orders were selected, I removed the outliers and normalised the data. When the data was prepared, I used SYSREM method to remove systematics, instrumental and electronic, telluric contamination and stellar signal, in order to have the signal from the planet free from other sources.

The atmosphere models used in this work was created by me using petitRADTRANS, using each planet's characteristics. I created atmosphere models of just one element avoiding deeper analysis due to the conditions of UHJs atmospheres.

Once I have the models and the planet data, I could apply the cross-correlation method, which correlates the signal from the planet with the models. This produced three different results: residuals, K_p map and the CCF, which are used for the analysis.

The analysed planets are HAT-P-57 b, KELT-17 b, KELT-21 b, WASP-189 b and HD 189733 b. I had a clear detection for the night 2019-01-26 of KELT-17 b where I found FeH with a significance of $\sim 4.8\sigma$, then for both nights , 2019-06-28 and 2019-06-23, from HAT-P-57 b I found water but with a low significance of $\sim 3.6\sigma$ and CO_2 with $\sim 4.7\sigma$, but I cannot claim them as detections due to the uncertainty of this planet's K_p and some losses of signal during the observation. For the res of the planets nothing was found.

In general, this work achieved its goals and even exceeded them, as we expected to get non-detections but obtained some positive discoveries that open the door for future studies.

Contents

1. Introduction

1.1. History of exoplanets

Since the dawn of science, human beings have pictured other planets and civilizations, and now we have enough information to know the different kinds of planets that we can find in outer space.

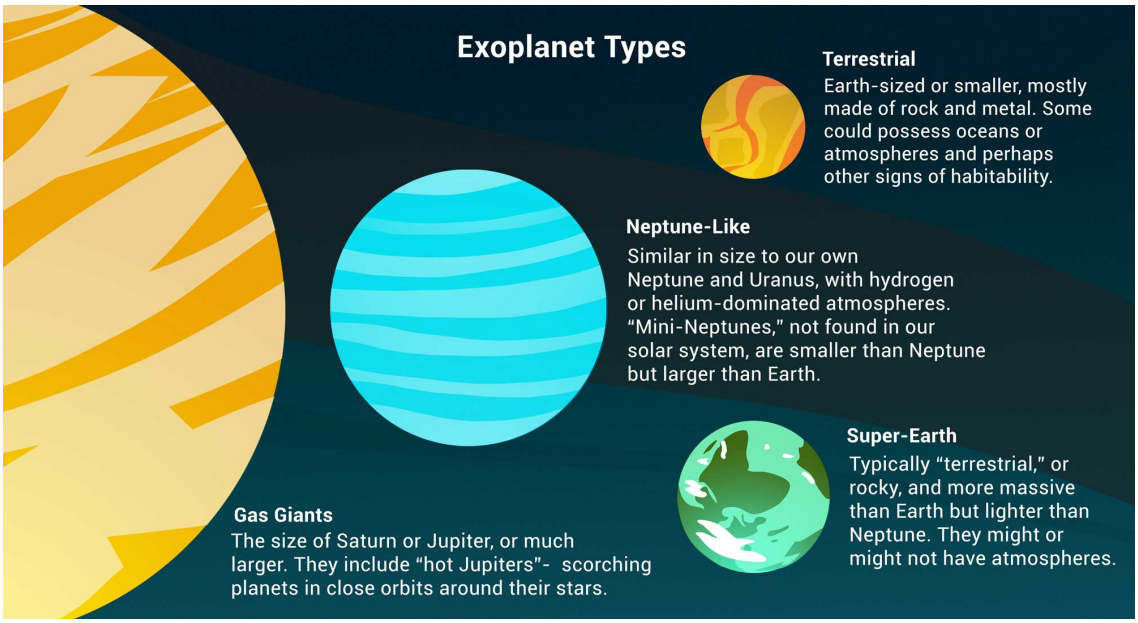

Figure 1: Illustration of the different main types of planets known at the time of writing NASA.

As shown in Fig. 1, there are many different kinds of worlds. We initially thought the normal distribution for planets in a planetary system was the solar system's. The system was formed from a gas and dust cloud which collapses into a planetary disk. The rocky and small planets should be closer to the star, due to the absence of ice and the small size of the feeding zone that causes the rocky planets to have smaller cores. The outer parts of the protoplanetary disk, beyond the snow line, should be occupied by great rocky cores in large feeding zones with plenty of gas and ice and thanks to the size of their nuclei they could accrete that gas and ice. This theory was based on an observational sample of our Solar System, being consistent until hot Jupiters were discovered orbiting a main sequence star. The first one was 51-Pegasi-b (Mayor and Queloz [1995]), officially named Dimidium.

When it was discovered it upended the typical solar system picture we had created. It was a gas giant planet with a close-in orbit. Its orbit is 10 times closer than Mercury's one. This was not the first time that someone postulated this theory, in 1952 Struve [Struve, 1952] proposed new methods to study radial velocities, and in that proposal, he mentioned the possibility of the existence of Jupiter-size planets orbiting close to their star as an explanation for the loss of angular momentum in some studied stars. However, it was not completely confirmed until the discovery of the first exoplanet.

Thanks to this discovery, we established the limits that help us to classify exoplanets. A planet will be taken as a hot Jupiter if its mass is at least $0.25\mathrm{M_J}$ and its orbital period is shorter than 10 days, which means a very close-in orbit and, consequently, a high equilibrium temperature, normally over $800\,\mathrm{K}$. Nowadays, another kind of planet is distinguished, the ultra-hot Jupiters, they have the same

mass limit but their period is lower than a day or they are orbiting a hot star, which is traduced in a equilobrium temperature over $2000\,\mathrm{K}$.

As mentioned before, since 1952, there were ideas about how to attack the problem of planet detection and radial velocity calculation, these ideas were based on the eclipses. While a planet is in a co-planar orbit concerning its star, it could incline respect to us, so if we want to detect a planet, we should observe the evolution of the lightcurve of a star looking for a change in depth. For that, we need the inclination of the orbit to be near $90°$.

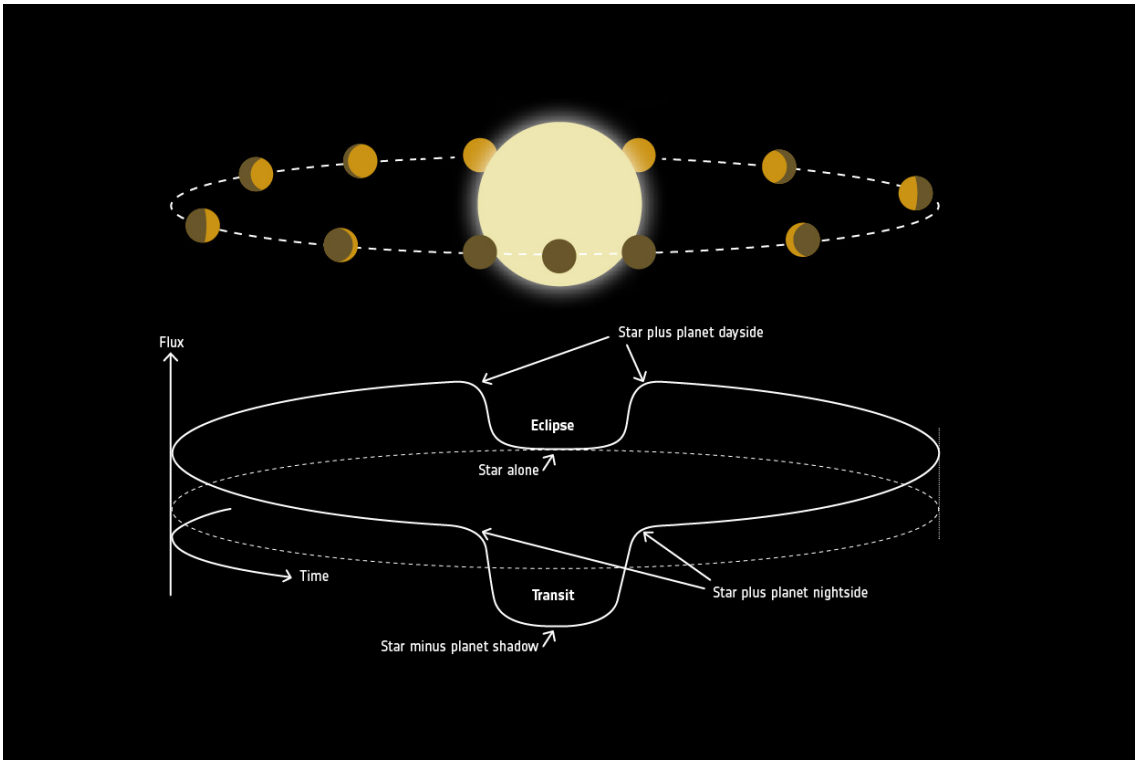

Figure 2: Variation of flux observed from a star over the phase of a transiting exoplanet, including the primary transit and the secondary eclipse. Diagram from ESA.

As shown in Fig. 2, the planet will overshadow the star, so we are going to detect a loss of signal in the star's lightcurve, which is represented at the bottom of the image. If we follow this reasoning, it is easy to realise that the bigger and closer the planet is to the star, the easier we will notice its existence. It is for that reason that the first ever discovered exoplanet was a hot Jupiter, they are the most likely to be detected.

1.2. Hot Jupiter Formation

Once the typical picture of a planetary system was completely erased due to the existence of these planets, we tried to find an explanation for their existence and formation.

There are three main theories (Dawson and Johnson [2018]). In situ, formation, which depends on two main mechanisms proposed for giant planet formation; the gravitational instability near the star, which is not plausible due to the high temperature that the gas reaches close to the star, in the accretion disk, would unbind the gas from the star (Rafikov [2005]); and the Core accretion, this is not feasible due to the high mass of solids the core has to reach (Rafikov [2006]).

Gas disk migration, which means that the torques from the protoplanetary disk can shrink a giant planet's semi-major axis from several astronomical units to hundredths of an astronomical unit, is caused by an exchange of angular momentum between the planet and the disk in which the planet perturbs nearby gas onto horseshoe orbits and deflecting more distant gas. There are two different types of migrations, nevertheless, the one that is of interest is the type II migration, which happens when a planet is massive enough to open a gap in the disk by deflecting it.

High-eccentricity tidal migration, unlike the gas disk migration, is based on a two-step process, the first step consists of a perturber extracting orbital angular momentum from the Jupiter by perturbing the Jupiter onto a highly elliptical orbit, and the second step in which the Jupiter tidally dissipates its orbital energy through interactions with the central star.

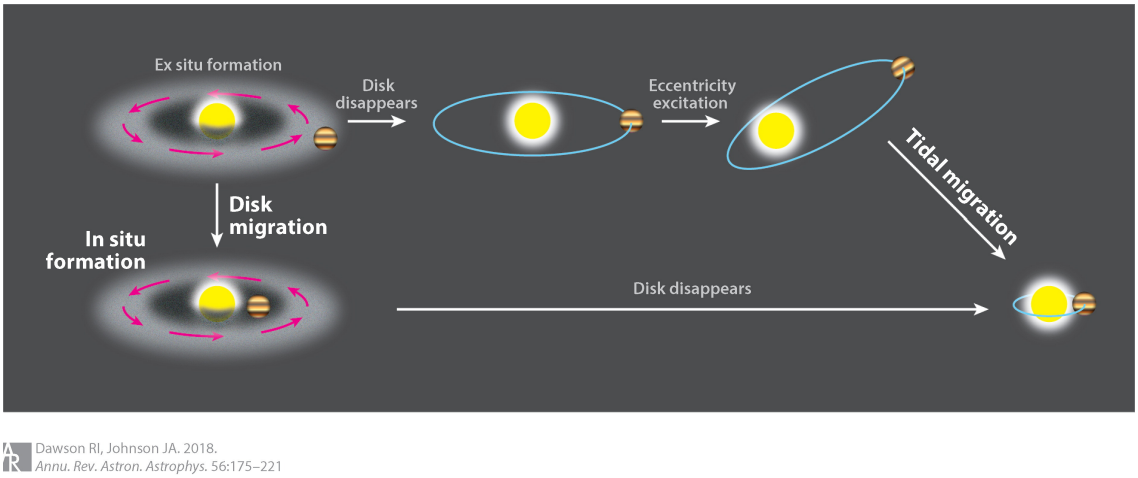

Figure 3: Dawson and Johnson [2018] Schematic summary of the three theories of hot Jupiter formation.

1.3. Hot Jupiter atmospheres

As you can see in Fig. 3, all of these theories drive us to the same point, a violent environment inside the planet. Normally, the atmospheres of hot Jupiters are completely affected by strong incident radiation, large horizontal temperature contrasts, species in the ionic, atomic, molecular, and condensate phases, and fast winds that approach or exceed the speed of sound [Fortney et al., 2021]. All of these, are caused by the proximity to the host star. On the other hand, their proximity causes a short orbital period that allows us to characterise them in a complete orbital phase.

Due to these hostile conditions, it is unlikely that we can find molecules in their atmospheres. The most normal elements found in the hottest hot Jupiters' characterisation are Fe, He, K, and Na in the optical range due to the opacity dominance they have in this range, like in a typical M-type or late K-type star. However, some molecular bands could be found in different scenarios, bands like VO and TiO. Nowadays, studies done in the NIR have found that the dominant carbon carrier in hot Jupiter is CO, in the case of nitrogen is N_2, and oxygen is only found in CO and H_2O. Other molecules that can be found but are more related to kinetic chemistry are HCN, C_2H_2 and O_2. [Fortney et al., 2021].

Using this chemical information and the easiness that we have while studying these planets due to the shot orbital period and their atmosphere properties, hot Jupiters were the first planets to be

characterised using transmission spectroscopy.

1.4. High-resolution transmission spectroscopy

Since we have know the existence of exoplanets we have wanted to open the door of studying their atmospheres. In the early 2000s, we made the first step in this in studies like Charbonneau et al. [2002], Brown [2001a], and Seager and Sasselov [2000] where we were able to study them using transmission spectroscopy. Which is based on the imprint that the planet terminators leave in the stellar signal when the starlight passes through the planet during the transit.

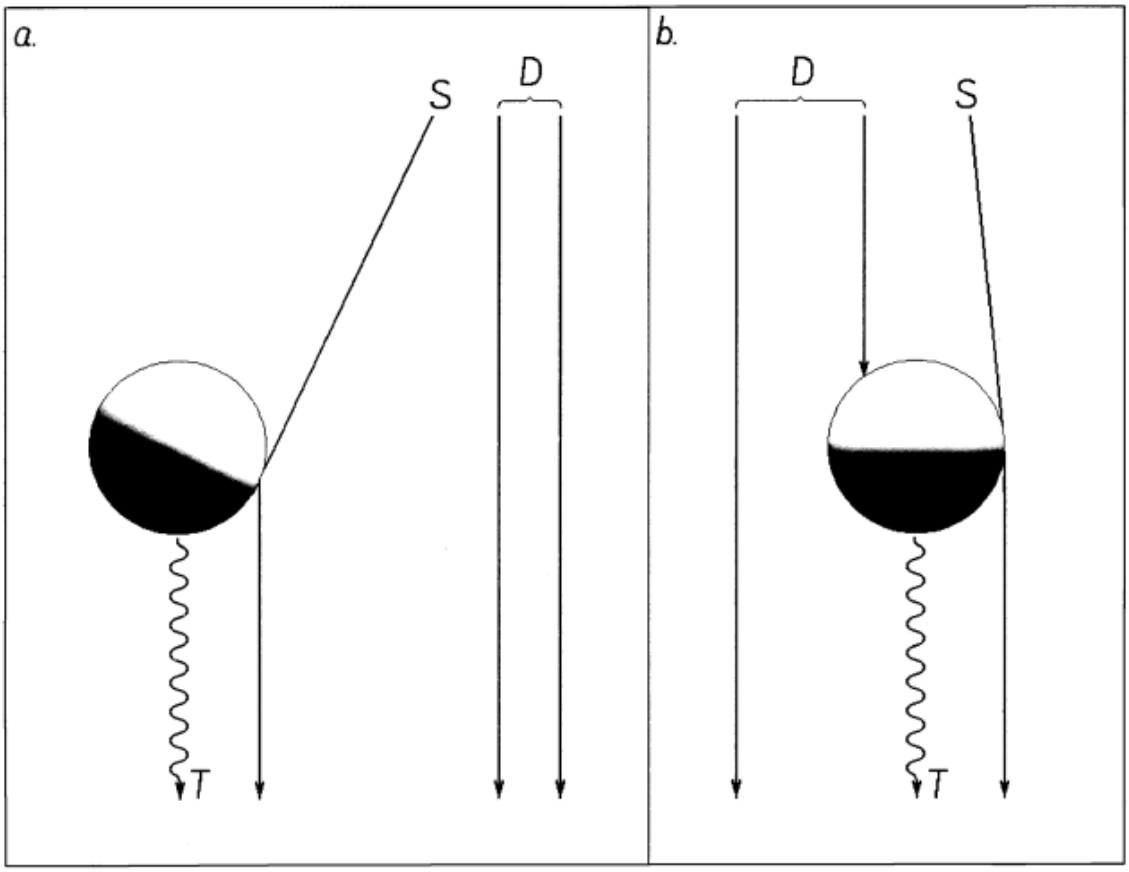

Figure 4: Brown [2001b] Scheme of the sources of transmission that come to the observer during a transit. Direct signal from the star (D), thermal radiation from the planet (T) and scattered signal (S).

These first studies were made using low-resolution transmission spectroscopy, in Brown [2001a] they had a resolution of $\mathrm{R} = 5540$, they only could look for wide bands like sodium bands.

It was not until 2010 with Snellen et al. [2010] that we got a suitable method that could carry us to studying them with high-resolution spectroscopy, until that moment we were only able to study them using low-resolution transmission spectroscopy.

In that paper, they introduce a method based on the cross-correlation of the signal obtained from the planet transmission and the theoretical transmission model of the different molecules they studied, but this is not that easy. First of all, not all planets can be studied with this method, but we need to know the host star's radial velocity and then, mass and radius, if we know all of this we can calculate the planet's parameters (the period, the systemic velocity, the orbital phase value in which transit happens

and the radial velocity semi-amplitude). Once we detect the transit and apply photometric analysis to get all the system parameters, we can use the target for this high-resolution method.

After observing a transit, not all the spectra are useful, as explained in Fig. 2, if we need the transmission spectrum of the planet we can only analyse the frames where the planet's signal is overlapped with the star signal. In that way, we get the starlight filtered by the atmosphere of the planet which leaves an imprint of the molecules that form it.

While applying this method for the first time, Snellen et al. [2010] observe that one of the most important parts is to be careful about the Earth's atmosphere. Due to its composition and the clouds, the telluric contamination of the Earth is so strong that if you do not remove it with a good method you may remove the planet's signal. If not, the residuals of the cross-correlation will be completely dominated by telluric contamination. They solved this during the normalisation process by using telluric models and subtracting it from the spectra, they still found some traces of telluric contamination in the residuals so they removed these remaining residuals by fitting the variation in each pixel to the residuals determined in a strong water and a strong methane line. Thereafter, remaining low-frequency variations were removed by fitting a second-order polynomial to each spectrum. In addition, each pixel value was divided by its standard deviation over time. This last step reduces the influence of noisy parts of the spectra on the cross-correlation signal.

Thanks to this method several discoveries have been made, in Snellen et al. [2010] they discovered traces of CO in HD 209458 b, a hot Jupiter, using CRIRES, not the most important but the first one. Other important discoveries using this method are the one mentioned in Birkby et al. [2013] where they made a detection of water with a significance of 4.8σ which increased until 5.1σ when including CO_2 in the template, this detection is important because it is the first time that complex molecules were detected using ground-based telescopes even in highly telluric contaminated regions of the Earth and the detection of H_2O in 51 Peg b Mayor and Queloz [1995], another hot Jupiter, again using CRIRES, the significance of this detection is 5.6σ and no carbon-bearing molecules were detected, the importance of this arise from the detection of water in the first ever detected exoplanet.

After mentioning the most important detection thanks to cross-correlation I have to name the detections related to my work. These detections are the mentioned in Stangret et al. [2020], Stangret et al. [2021] and Stangret et al. [2022]. Each of these scholarly articles employs the specified method to investigate the atmosphere of ultra-hot Jupiters. The relevance of these studies to my work lies in the algorithm they use and how they process the data, both of which are grounded in the foundational code used in these papers. Some differences are going to be shown in Sect. 3, like the range of work, I am looking at NIR; in those works, they were working on visible range and the resolution of the instruments, they worked with HARPS-N, HARPS-S and EXPRESSO which have a resolution of $R\ 85000 - 100000$: Higher than the one I have in GIANO-B and the last difference is that they were taking in account the Rossiter-MachLaughlin effect, which I decided not to include into my analysis.

That is why my data treatment had to be stronger than what they did in their works, to avoid all the noise my atmosphere provokes in the NIR and the problems that GIANO-B has, which are mentioned in Sect. 3.

Apart from the similarities between my work and theirs, they get some different results in each

case, in Stangret et al. [2020] they looked for Fe I and Fe II in the visible range on MASCARA-2 b, they found clear evidence of the presence of Iron in that atmosphere with a combined significance of 10.5 ± 0.4 for Fe I and 8.6 ± 0.5 for Fe II; in Stangret et al. [2022] they found nothing due to the high surface gravity of MASCARA-5 b and in Stangret et al. [2021], which is the most related paper to my work due to the planets they studied, they found Fe I with a significance of 5.1σ, Fe II with 5.4σ and Ti I with 4.2σ in WASP-189 b, for the other 5 planets, KELT-7 b, KELT-17 b, KELT-21 b, HAT-P-57 b, and MASCARA-1 b, they did not find anything due to high surface gravity and the high brightness of the host star. My work centres on studying these planets to check if the behaviour of their atmospheres keeps in the NIR. This last paper is the most important for us, due to is the one I took as a first approach to apply cross-correlation using GIANO-B data and my idea is to review the results for the same planets as they did but in the NIR.

Other method to analyse High-Resolution Spectra, is single line's fitting, applied in Casasayas-Barris et al. [2017] and Casasayas-Barris et al. [2020]. Our work is related to this one due to the original code was thought to be applied for these methods, after that in Stangret et al. [2020], Stangret et al. [2021] and Stangret et al. [2022] they took the reduction part of the original code to imply it in the cross-correlation process and I took this and improve it to be applicable for NIR data.

1.5. GIANO-B

GIANO-B is a near-infrared echelle spectrograph that is mounted in the TNG (Telescopio Nazionale Galileo), an altazimuth telescope with a Ritche-Chretien optical configuration and a flat tertiary mirror feeding two opposite Nasmyth foci.

One of the main strengths of the TNG is the Active Optics systems, providing real-time low-frequency corrections to ensure the best optical performances to compensate for the deformations of the primary mirror. This system works by using two Shack-Hartman wavefront sensors to measure wavefront deformations using an off-axis star. This data helps me correct the optical surface of the primary mirror and the positions of the secondary and tertiary mirrors.

TNG is equipped with SiFAP2, HARPS-N, Nics, Dolores, and GIANO-B, the last one is the one which I have worked with.

GIANO-B has an optical design based on three mirrors anastigmat combination used in a double-pass, they have the same effect as a collimator and a camera. The dispersing element is an echelle grating working at a fixed position in a quasi-Littrow configuration with an off-axis angle along the slit of 5. It also has a cross-disperser consisting of a system of prisms from high-dispersing IR optical materials. It includes a two-mirror system that re-images the slit far from any problematic element due to the entrance image of this system lying close to the detector. (Oliva et al. [2012])

This spectrograph works at a resolution of 50000, covering a spectral range from $0.9\,\mu\mathrm{m}$ to $2.45\,\mu\mathrm{m}$ in a single exposure. The components that make possible this are a cold slit with on-sky dimensions of $6" \times 0.5"$, located inside the spectrograph's cryogenic dewar; the HAWAII-2 2048×2048 array, which has a pixel scale of $18\,\mu\mathrm{m}$, $0.25"$ on the sky, a readout noise of $5\,\mathrm{e^-/px}$, a gain of $2.2\,\mathrm{e^-/ADU}$, a Dark current of $0.05\,\mathrm{e^-/s/px}$ and a resolution element of $2\,\mathrm{px}$ for $0.5"$ slit; the auto guider, mechanically coupled with the spectrograph dewar.

These features open a world of possibilities, as seen in GIANO Whitebook and in Oliva et al. [2012], like observation of rocky exoplanets, due to the capability of GIANO-B to measure a large number of NIR features at high resolution; low mass stars and brown dwarves observations due to the broad continuum spectral coverage in the NIR that GIANO-B provide; analysing star-forming regions by studying the velocity structure of the usual emission lines of these regions to obtain information on accretion/ejection mechanism and on the activity of low mass young stars out from the MS; analysing cold stellar atmospheres, the combination of high spectral resolution and broadspectral coverage make me able to obtain abundances of atomic species, to measure magnetic fields and mass loss activity of cold stars; studying extragalactic stellar clusters, as GIANO-B gives me NIR integrated spectra pf stellar clusters of the Local Group and beyond, this allows me to calculate their chemical composition and dynamical mass and study the star formation history and chemical enrichment of the host galaxy; estimating the Initial Mass Function (IMF) in starburst by resolving the width of absorption and emission lines in dust embedded Super Star Clusters I can constrain their dynamical mass and IMF; look into damped Lyman alpha systems, GIANO-B allow me to establish the metallicity of high redshift systems by appraising the the equivalent width of the associated absorption by variome atomic lines, which are shifted into the NIR.

Despite all these good characteristics, there are some problems with GIANO-B. Some of the spectral orders are problematic, I should discard the bluest and the reddest orders, these are due to overlapping signals, instabilities, and loss of signal. However, there are other risky orders due to hot and cold pixels, the way I dealt with these orders and how I discarded the orders will be explained in the methodology Sect. (3).

2. Objectives

The objectives of my work were to learn how exoplanet atmospheres can be studied using high-resolution cross-correlation spectroscopy, how to model theoretical spectra of planets, to create my own data reduction and cross-correlation pipeline for NIR spectra observed with the GIANO-B instrument, and, finally, to use the pipeline to study the atmospheres of a selection of hot Jupiters observed with GIANO-B.

The objectives can be divided into two main work packages (WPs), that were:

1. to adapt a high-resolution cross-correlation spectroscopy analysis pipeline developed for optical HARPS-N spectroscopy by Dr. M. Stangret [Stangret et al., 2020, 2021, 2022] to be used with GIANO-B spectroscopy observed in NIR; and

2. to apply the pipeline to previously unstudied GIANO-B transmission spectroscopy observations in order to search for signatures of molecules in hot Jupiter atmospheres.

The first WP required me to learn the steps for cross-correlation transmission spectroscopy, develop my programming skills, understand both optical HARPS-N and NIR GIANO-B spectroscopy data, and learn the different kinds of systematics that can affect the observations. The original HARPS-N pipeline was written in Python as Jupyter notebooks. I first had to understand how the HARPS-N

pipeline works and how to use all the Python packages (numpy, scipy, astropy, etc.) which were used by the pipeline. After this, I had to learn how the GIANO-B spectroscopy differed from the HARPS-N data so that I could adapt the pipeline. Finally, I had to modify the pipeline to work with GIANO-B data. This was a significant amount of work because the HARPS and GIANO-B data were different and required many of the reduction and analysis steps to be changed.

The second WP was all about science. I needed to learn what molecules we can expect to find in hot Jupiter atmospheres, how to create theoretical model spectra for cross-correlation, and how to interpret the results from my GIANO-B cross-correlation pipeline. Here, I studied four out of six planets studied by Stangret et al. [2021]: HAT-P-57 b, KELT-17 b, KELT-21 b and WASP-189 b. Stangret et al. [2021] studied the planets in optical using HARPS-N, and I wanted to see what I could find using NIR spectra obtained with GIANO-B. In addition to the four planets, I also tried to analyse and characterise HD 189733 b. This planet is hard to study as shown in Brogi et al. [2016] due to a strong Rossiter–McLaughlin effect (an effect I am not including in my analysis), and vertical winds, but I include the analysis here to compare the difficulties and differences I found during its analysis.

3. Methods

The methodology I followed for this project is based on that discussed in Sect. 1.4, Birkby et al. [2013, 2017] and Stangret et al. [2021]. First, I created the atmosphere models using Mollière et al. [2019] and taking into account the ultra-hot and hot Jupiters theory introduced in Sect. 1.2 . After that, I reduced the data and I made the data treatment in order to improve the quality of my results. Additionally, I used SYSREM to remove systematics from my data. And then I applied cross-correlation, for what I needed the planet data already reduced and the models I created.

The original data I used was reduced and calibrated by the Italian group from INAF, mainly by Mario Basilicata, using GOFIO and GUIBRUSH, developed by Paolo Giacobbe.

3.1. Atmosphere modelling

I created my atmosphere models using petitRADTRANS [Mollière et al., 2019]. The package takes a molecule template and the planet's atmospheric and physical parameters, to model the planet's atmosphere. The model is returned as two arrays, one for the wavelength and the other for the planet's radius as a function of wavelength.

In my case, I modelled atmospheres made of H_2O, CO, CO_2, CH_4, HCN and FeH, which are the most commonly found molecules in the NIR. Additionally, as I have access to ExoAtmospheres, IAC community database for exoplanet atmospheric observations, I have determined which are the most probable species that could produce a positive result during my analysis.

For each molecule for each planet, I created a model, Figs. 5 and 6 based on the tutorial of petitRADTRANS using the equilibrium temperature of each planet and taking solar abundances [Asplund et al., 2009] for each molecule.

For the first part, I use the RADTRANS package to get the high-resolution template of each molecule, I define my pressure array from -10 to 2. After this, I chose the molecule I wanted

to generate the template for, I ignored the the parameters of rayleigh species and gas continuum contributors because their contribution is negligible on these planets. I defined a broader wavelength range for the model than the data's range due to the cross-correlation process requirements. The model made has a resolution of 1000000.

After establishing this, I have to set the planetary parameters for each planet. Parameters like the planet's radius, mass, gravity, temperature and the mass fraction of each molecule. So the target must be well-known.

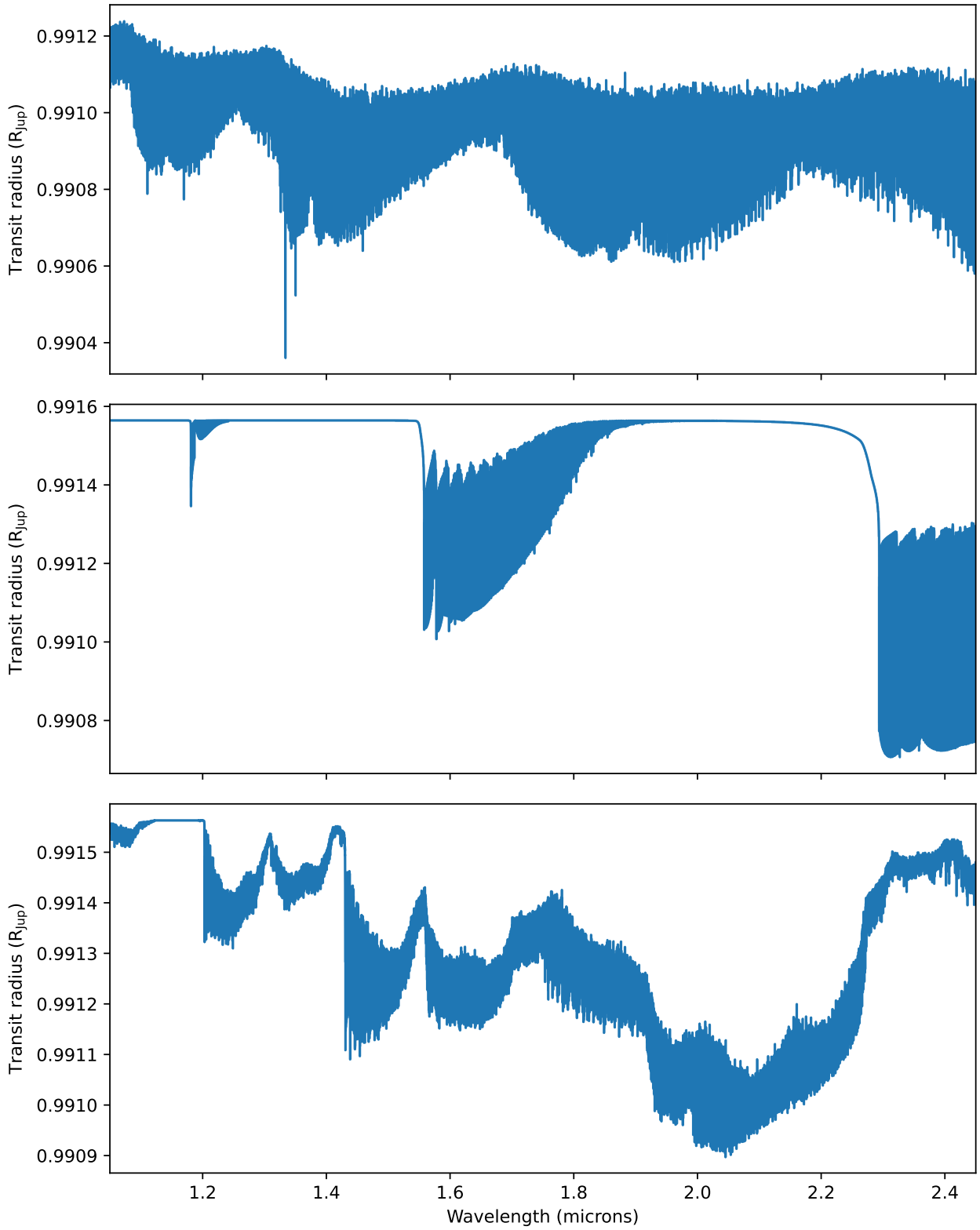

Figure 5: Model of a water-based, CO-based and CO_2-based atmospheres for HAT-P-57 b created using petitRADTRANS.

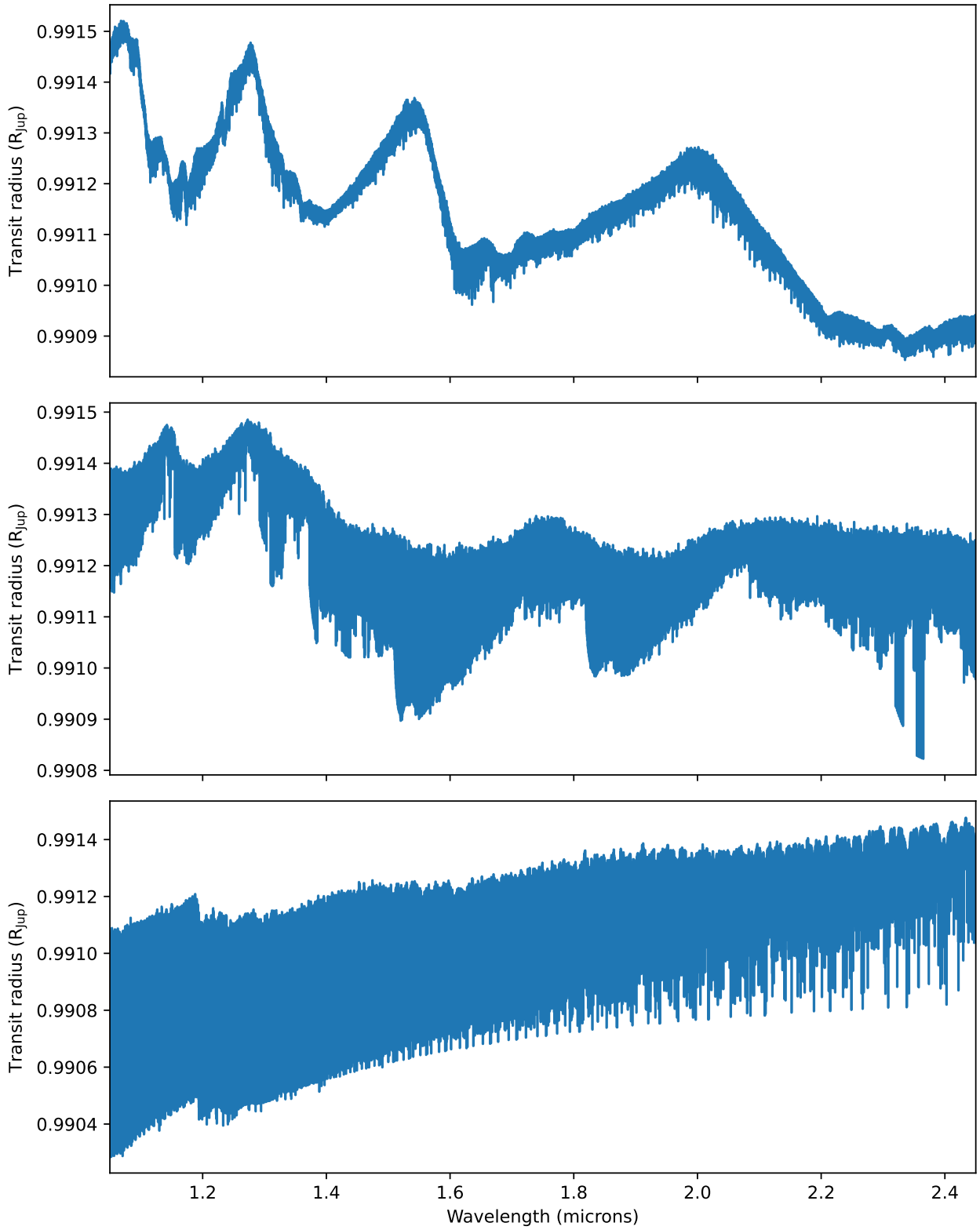

Figure 6: Model of a methane-based, HCN-based, and FeH-based atmosphere for HAT-P-57 b created using petitRADTRANS.

3.2. Cross correlation pipeline

3.2.1. Overview

My GIANO-B reduction and cross-correlation pipeline is based on Dr. M. Stangret's HARPS-N pipeline. It is written in Python as Jupyter Notebooks and considers the steps of order selection, removal of bad pixels, spectrum normalisation, systematic correction with SYSREM, and cross-correlation.

3.2.2. Data

The input data for my pipeline consists of a spectroscopic time series stored as a 3D array with a shape (order, exposure, wavelength) and additional information such as the orbital phase for each exposure. The data cube is produced from the raw exposures by my collaborators using the nodding ABAB configuration, allowing an optimal subtraction of the detector noise and background. GOFIO was used as a data reduction pipeline developed for GIANO-B, introduced in Rainer et al. [2018].

In this case, the offline version was used, it allows the user to work on an already completed night. The main features of GOFIO are the possibility of allowing to extract optimally the signals A and B from each nodding pair, flat corrected, with a signal-to-noise ratio for each pixel of each spectrum and it also provides a preliminary wavelength calibration calculated with lamps of U-Ne. This is not good enough to be the definitive calibration, GUIbrush code is used (Not the Monkey Island one), a GUI interface developed by Paolo Giacobbe and Francesco Amadori. GUIbrush is made of many codes, in our case we are only using four of them to re-calibrate the wavelength solution.

The first code extracts data and useful header information from the reduced data (e.g. airmass, SNR, etc); plots the SNR as shown in Fig. 7; organises the data as a cube (i.e. $50\,\mathrm{Spectral\,Orders} \times 52\,\mathrm{frames} \times 2048\,\mathrm{px}$); and produces a file with the wavelength solution provided by GOFIO (i.e. a matrix of $50\,\mathrm{Spectral\,Orders} \times 2048\,\mathrm{px}$).

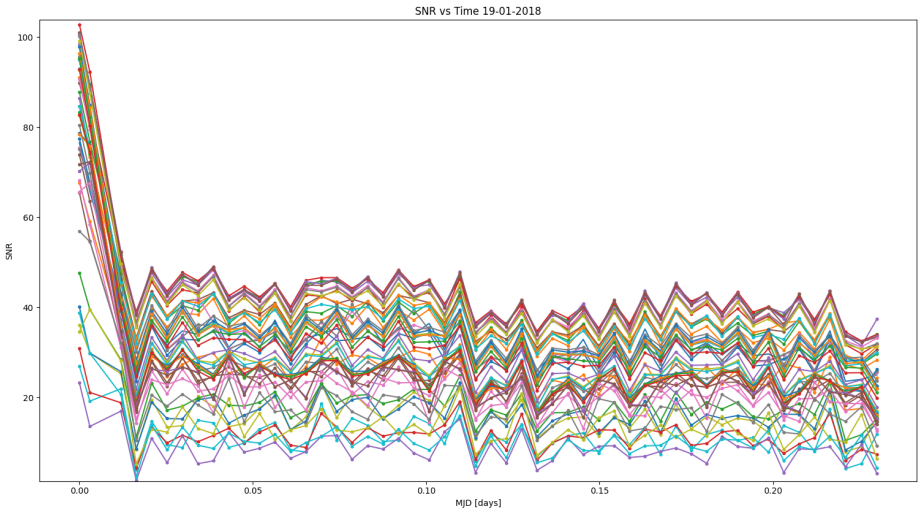

Figure 7: Dawson and Johnson [2018] Example of the SNR plot generated by GOFIO. This belongs to WASP127-b.

The second code computes the planetary orbital phase associated with each frame and the Earth barycentric correction, for I need the planetary system's parameters(i.e. the transit epoch, the period, the systemic velocity, the orbital phase value in which transit happens and the radial velocity semi-amplitude) for the cross-correlation analysis.

The third code aligns each spectra of a single spectral order to the mean spectrum (in that order) and repeats this procedure for each order, this is necessary due to the drift of the spectra on the GIANO-B detector. The produced file contains the cube of the aligned spectra which will be used for the cross-correlation function analysis. It also creates a file made from 50 plots, in which I can see the drift of each spectrum, Fig. 8, for each spectral order, concerning the mean spectrum.

The fourth code, repeats the wavelength calibration in a more precise way (using a template of the telluric lines) and produces a file with the refined wavelength solution, which will be used to compute the CCFs.

3.2.3. Selection of orders

The cross-correlation analysis begins with the removal of bad spectroscopy orders. These problematic orders appear due to GIANO-B's problems mentioned in Sect.1.5. I identified them thanks to images like Figs. 8 and 7.

After the pipeline shows the "raw" data, I checked it as in Fig. 9, where I can detect these problematic orders, frames, or pixels. With the information provided by Figs. 8 and 7, I made an initial selection. The result of this selection is shown in Fig. 10. Once I made the initial selection, I removed the orders saturated by telluric absorption.

3.2.4. Removal of hot and cold pixels

Removing bad orders is an important first step, but some orders still have hot and cold pixels. As the next step, the pipeline identifies hot and cold pixels and replaces them with the median value of the neighbouring pixels. The choice of a median filter over a polynomial fitting, used by Dr. M. Stangret, is based on the extremely high values that some hot pixels reached which made impossible the performance of a polynomial fitting.

The pipeline first removes the running median from a spectrum and then identifies the outliers based on the scatter of the residuals. Points deviating more than $5\,\sigma$ are considered outliers and values below 1 are considered cold pixels. I used this last criterion to avoid instabilities when the normalisation algorithm is applied. These instabilities are created due to the flat correction process that the Italian group makes. Instead of dividing the raw data by the flat combined during the first reduction process, they subtract it, which causes extra-cold pixels, below -40, to appear.

3.2.5. Spectrum normalisation

After removing outliers, the pipeline normalises the data by splitting each order into 50 parts and taking the 50 highest values of each division. With these values, it creates a polynomial that fits them

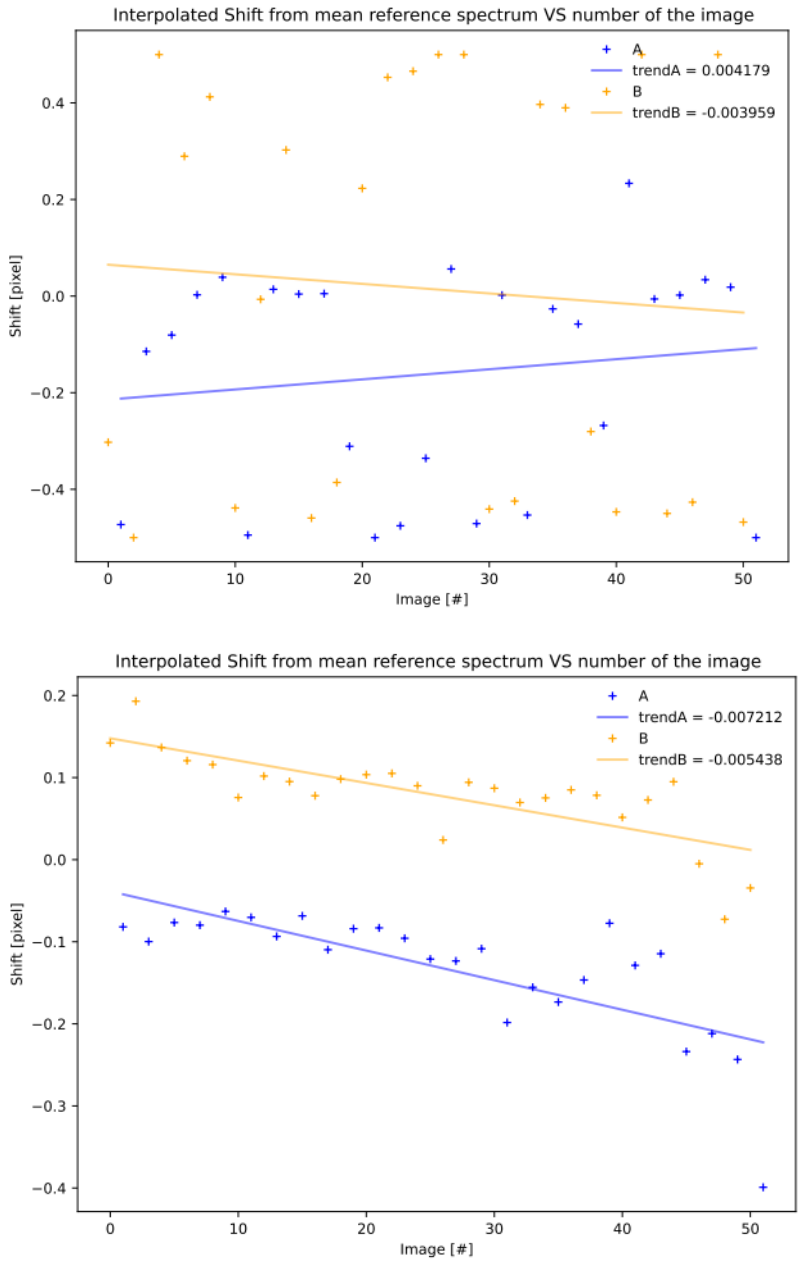

Figure 8: Example of the drift plot generated by GOFIO. The spectra belonging to the nodding positions A and B are plotted with two different colours to see differences in the drift of spectra taken in the two nodding positions. If the observation for an order is good (image 2), the drift of each order should be parallel between A and B, and well defined, if not (image 2), the points spread all over and the data turns bad.

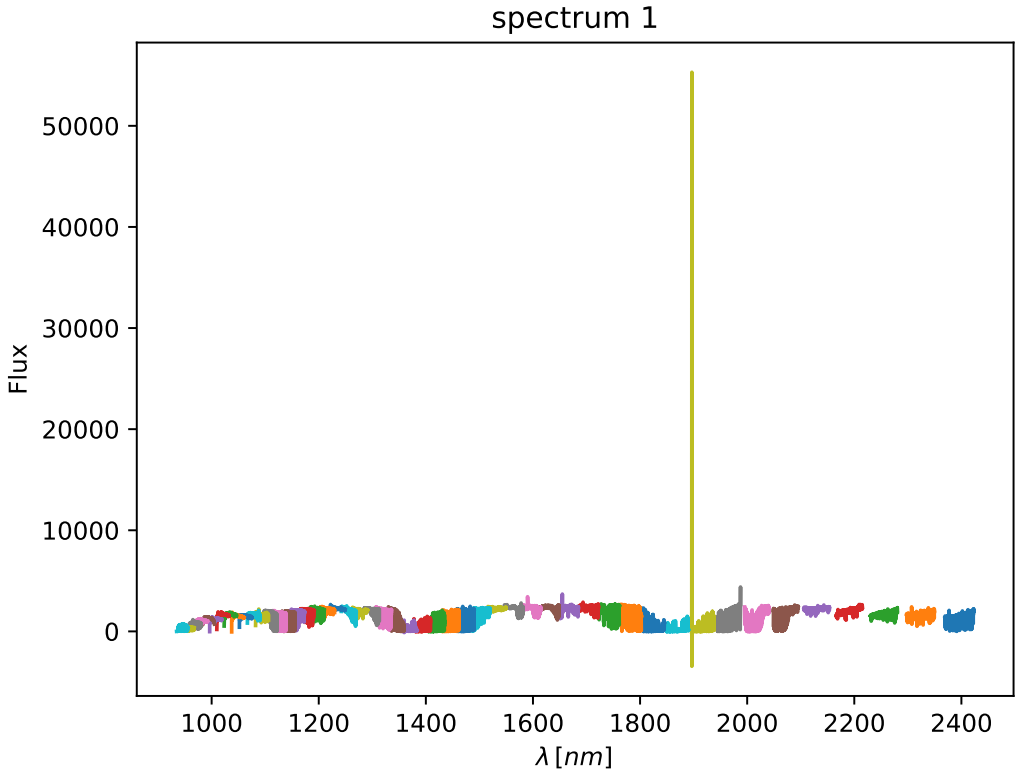

Figure 9: First complete raw spectrum of WASP127-b. Each colour represents a different order. An outlier could be seen in the middle of the spectrum and also in the saturated telluric bands.

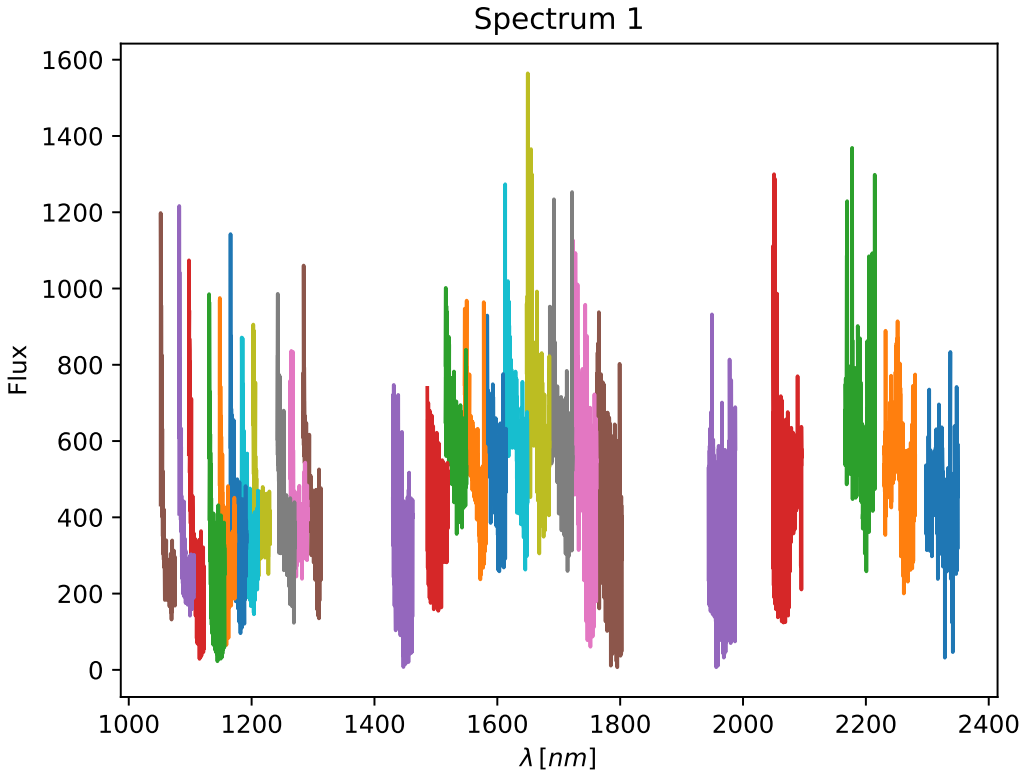

Figure 10: Same spectrum as in Fig. 9, with the problematic orders removed. Here, the order with the outlier was removed and the saturated orders were also removed.

with the wavelength. After this, the pipeline divides each order by each polynomial fit to produce a normalised spectrum with long-term trends removed.

3.2.6. Removal of systematics with SYSREM

Once the spectra are well-reduced, the pipeline applies SYSREM to correct systematic errors. Systematic errors are induced by sources that produce noise correlated in time but can be independent of wavelength. Normally, due to instrument calibration, sensitivity, and precision. However, systematics in astrophysics are not limited to instrument-induced errors; they can also arise from various other sources. For example, in my work, the telluric contamination and the stellar signal are considered systematic effects. My goal is to identify, understand, and minimise these errors to ensure the accuracy and reliability of my results.

As it is impossible to prevent observations from systematics, I used SYSREM to improve the quality of my data. I chose SYSREM over other methods to remove the systematic effects, telluric contamination, and stellar signal, due to the simplicity of this algorithm which allows me to correct my normalised data without any prior knowledge of the underlying cause.

SYSREM, is an algorithm based on Principle Component Analysis (PCA) but also allows for unequal error bars per data point, and it was released on Tamuz et al. [2005].

For the application of this algorithm, I based it on previous studies like Birkby et al. [2013, 2017]. The functioning of this process is explained in Sect. 2.3 of those papers. As expected, I also based on Stangret et al. [2020, 2021, 2022] and how they apply this algorithm.

This code was created for ground-based wide-field transit surveys to correct systematic effects common to all light curves [Collier Cameron et al., 2006]. However, they discovered its utility in removing telluric contamination and the star signal from the in-transit data frames due to the stationary signal that both caused during the observations. You may think that the planet's signal should also be stationary, but the spectral fingerprint of the planetary atmosphere tilts due to its velocity, so it is not removed.

This step should be the last before applying the cross-correlation to facilitate SYSREM's work. The first systematic component removed by SYSREM is related to the airmass, and then it scales iteration by iteration. Normally, 8/9 iterations are enough for planetary atmosphere analysis but to have a broad catalogue of results to reach high SNR in the planet's signal, I ran 15 iterations and took only the highest SNR to provide the best possible result.

3.2.7. Cross-correlation

For cross-correlation, an atmosphere model and a well-reduced dataset are needed. Once I had it, the first thing I needed was to make the atmosphere model fit the format of our data as I told in Sect. 3.1. The resolution of the produced model is much higher than our data resolution and is not divided by orders. Due to this, I need to interpolate the model with the wavelength array to obtain the model divided into orders that can be introduced in the CCF, Fig. 11. After the interpolation, I normalised the model with the same method I used for my data to improve the efficiency of our CCF.

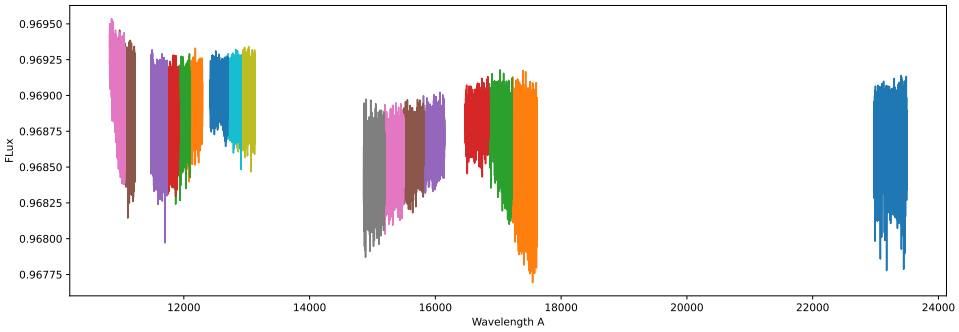

Figure 11: H_2O model created with petitRADTRANS cut in order to make it fit with our data.

After this, I loaded my SYSREM results, the highest SNR iteration, and defined an RV array based on Brogi et al. [2018], from -225 to $225\,\mathrm{km/s}$ with steps of $2.7\,\mathrm{km/s}$ calculated from the technical capabilities of GIANO-B, to use it with the pyAstronomy package crosscorrRV.

The result is a residual map of each order of each spectral frame, Fig. 12, where nothing can be seen separately. However, if they are summed some traces of the molecule along the time of the observation can be seen and I obtain a residual map of the whole observation.

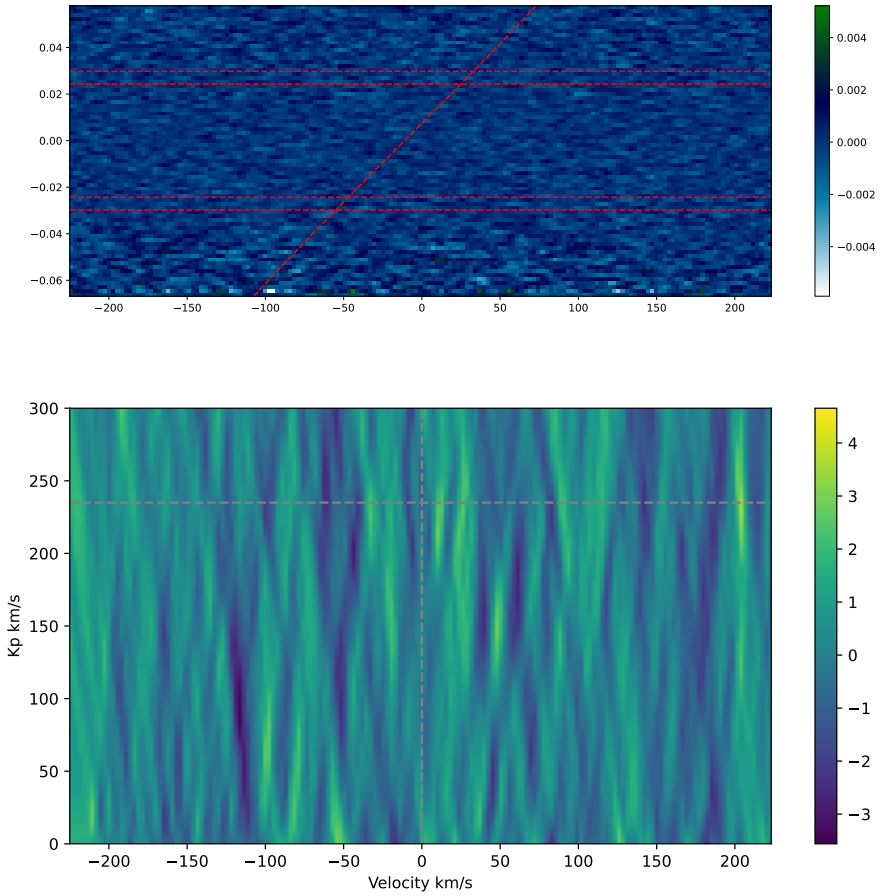

Figure 12: Residual map obtained after applying CCF to HAT-P-57 b data with H_2O model. second–K_p map obtained after applying CCF to HAT-P-57 b with H_2O model.

After that, I defined the spectral frames that are in-transit and out-of-transit, to get the result in

terms of SNR. Plotted it in a K_p map, Fig. 12. Here is where the detection must be clear.

4. Studied systems

I have chosen five different planets for analysis: 4 UHJs and 1 HJ. They are HAT-P-57 b, KELT-17 b, KELT-21 b, and WASP-189 b, mentioned in Sect. 2. I chose them due to my interest in continuing the work done by Dr. Stangret [Stangret et al., 2021] where they studied these planets in optical. I have also chosen HD 189733 b, a hot Jupiter, to show how different the results could be due to the hostile atmospheric conditions that these planets suffer due to their composition and proximity to the host star, i.e. for HD 189733 b it has strong vertical winds as discussed in Brogi et al. [2016].

Table 1: Stellar parameters.

Main identifiers	HAT-P-57	KELT-17	KELT-21
Equatorial Coordinates			
RA (J2000)	18:18:58.4	08:22:28.0	20:19:12.0
Dec (J2000)	+10:35:50.1	+13:44:07.0	+32:34:52.0
Stellar Parameters			
Spectral Type	A8V	A	A8V
$M_*[M_\odot]$	1.47 ± 0.12	1.635 ± 0.060	1.458 ± 0.028
$R_*[R_\odot]$	1.50 ± 0.05	1.645 ± 0.055	1.638 ± 0.034
$K_s[m/s]$	< 215.2	131 ± 34	< 399.6
$logg[dex]$	4.251 ± 0.018	4.220 ± 0.023	4.173 ± 0.014
$T_{\rm eff}[K]$	7500 ± 250	7454 ± 49	7598 ± 8

Main identifiers	WASP-189	HD 189733
Equatorial Coordinates		
RA (J2000)	15:02:44.9	20:00:43.0
Dec (J2000)	-03:01:52.9	+22:42:39.0
Stellar Parameters		
Spectral Type	A6IV-V	K1-K2
$M_*[M_\odot]$	2.030 ± 0.066	0.828 ± 0.028
$R_*[R_\odot]$	2.36 ± 0.03	0.805 ± 0.016
$K_s[m/s]$	182 ± 13	204.7 ± 2.6
$log_g[dex]$	3.9 ± 0.2	4.56 ± 0.03
$T_{eff}[K]$	7996 ± 99	4875 ± 43

Table 2: Planetary parameters.

Main identifiers	HAT-P-57 b	KELT-17 b	KELT-21 b
Orbital Period $[days]$	2.46529488	3.08017985	3.61276958
T_0 $[days]$	2457598.49926	2459440.791304	2458881.93965
M_{pl} $[M_J]$	1.41 ± 1.52	1.31 ± 0.28	< 3.91
R_{pl} $[R_J]$	1.413 ± 0.054	1.525 ± 0.062	1.586 ± 0.039
i $[°]$	88.26 ± 0.85	84.87 ± 0.44	86.46 ± 0.36
V_{sys} $[km/s]$	-9.6	28.0	-13.0
T_{14} $[hours]$	3.499	3.475	4.105
a $[AU]$	0.0406 ± 0.0011	0.04881 ± 0.00063	0.05224 ± 0.00034
K_p $[km/s]$	235 ± 254	171 ± 37	156 ± 72
T_{eq} $[K]$	2200 ± 76	2087 ± 32	2051 ± 29

Main identifiers	WASP-189 b	HD 189733 b
Orbital Period $[days]$	2.7240308	2.218574944
T_0 $[days]$	2456706.4566	2456194.067619
M_{pl} $[M_J]$	1.99 ± 0.15	1.130 ± 0.046
R_{pl} $[R_J]$	1.619 ± 0.021	1.142 ± 0.035
i $[°]$	84.03 ± 0.14	85.27 ± 0.23
V_{sys} $[km/s]$	-24.465	-2.204
T_{14} $[hours]$	4.3336	1.8264
a $[AU]$	0.05053 ± 0.00098	0.031
K_p $[km/s]$	195 ± 21	157 ± 9
T_{eq} $[K]$	3353 ± 31	1220 ± 13

The references for each system are:

1. HAT-P-57/HAT-P-57 b: OP and T_0 from Kokori et al. [2023]; RA, Dec, M_*, R_*, K_s, $\log_g$, T_{eff}, R_{pl}, i, T_{14}, a, and T_{eq} from Hartman et al. [2015]; M_{pl} from Jiang et al. [2023]; K_P derived from Stassun et al. [2017]; V_{sys} from Prusti et al. [2016], Brown et al. [2018], Cropper et al. [2018] and Katz et al. [2019]

2. KELT-17/KELT-17 b: OP and T_0 from Kokori et al. [2023]; RA, Dec, M_*, R_*, K_s, $\log_g$, T_{eff}, R_{pl}, i, T_{14}, a, and T_{eq}, M_{pl} and V_{sys} from Zhou et al. [2016]; K_P derived from Stassun et al. [2017]

3. KELT-21/KELT-21 b: OP and T_0 from Kokori et al. [2023]; RA, Dec, M_*, R_*, K_s, $\log_g$, T_{eff}, R_{pl}, i, T_{14}, a, and T_{eq}, M_{pl} and V_{sys} from Johnson et al. [2018]; K_P derived from Stassun et al. [2017]

4. WASP-189/WASP-189 b: OP from Ivshina and Winn [2022];T_0 from Kokori et al. [2023]; RA, Dec, M_*, R_*, K_s, $\log_g$, T_{eff}, R_{pl}, i, T_{14}, a, and T_{eq} from Lendl et al. [2020]; K_P derived from Stassun et al. [2017]

5. HD 189733/HD 189733 b: OP, T_0 and i from Kokori et al. [2023]; RA, Dec, R_*, $\log_g$, T_{eff}, R_{pl}, M_{pl}, T_{14}, a, and T_{eq} from Addison et al. [2019]; M_* from Rosenthal et al. [2021]; K_s from Paredes et al. [2021]; K_P derived from Stassun et al. [2017]

5. Results

In this section, I only show the most important results in order to avoid overloading the thesis with images with the same information. For all of the planets, we have studied H_2O, CO, CO_2, CH_4, HCN and FeH, mentioned in Sect. 3.1.

5.1. Detections

5.1.1. HAT-P-57 b

For this UHJ, I had data from two nights, 2019-06-28 and 2019-06-23. For the first night, I had 68 spectral frames distributed as seen in Fig. 13. I used only 17 out of 50 possible orders and the 5^{th} iteration of SYSREM. I found a signal of $\sim 3.6\sigma$ for water which you can see in Fig. 14, that will be discussed later.

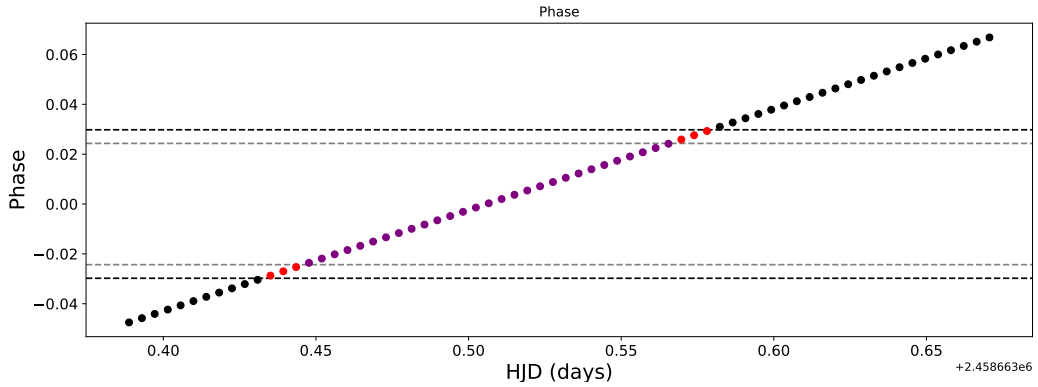

Figure 13: Diagram showing the orbital phase of HAT-P-57 b on 2019-06-28. Each dot represents a single spectral frame so this diagram shows the evolution in time of the planet's position. The black dashed lines represent the moments when the planets began and ended the transit, T_1 and T_4. The grey dashed lines show the moments when the planet's surface is completely inside and outside the star's surface, T_2 and T_3. The black points are the out-of-transit frames, the red ones are the beginning and end of the transit and the purple dots represent the in-transit frames.

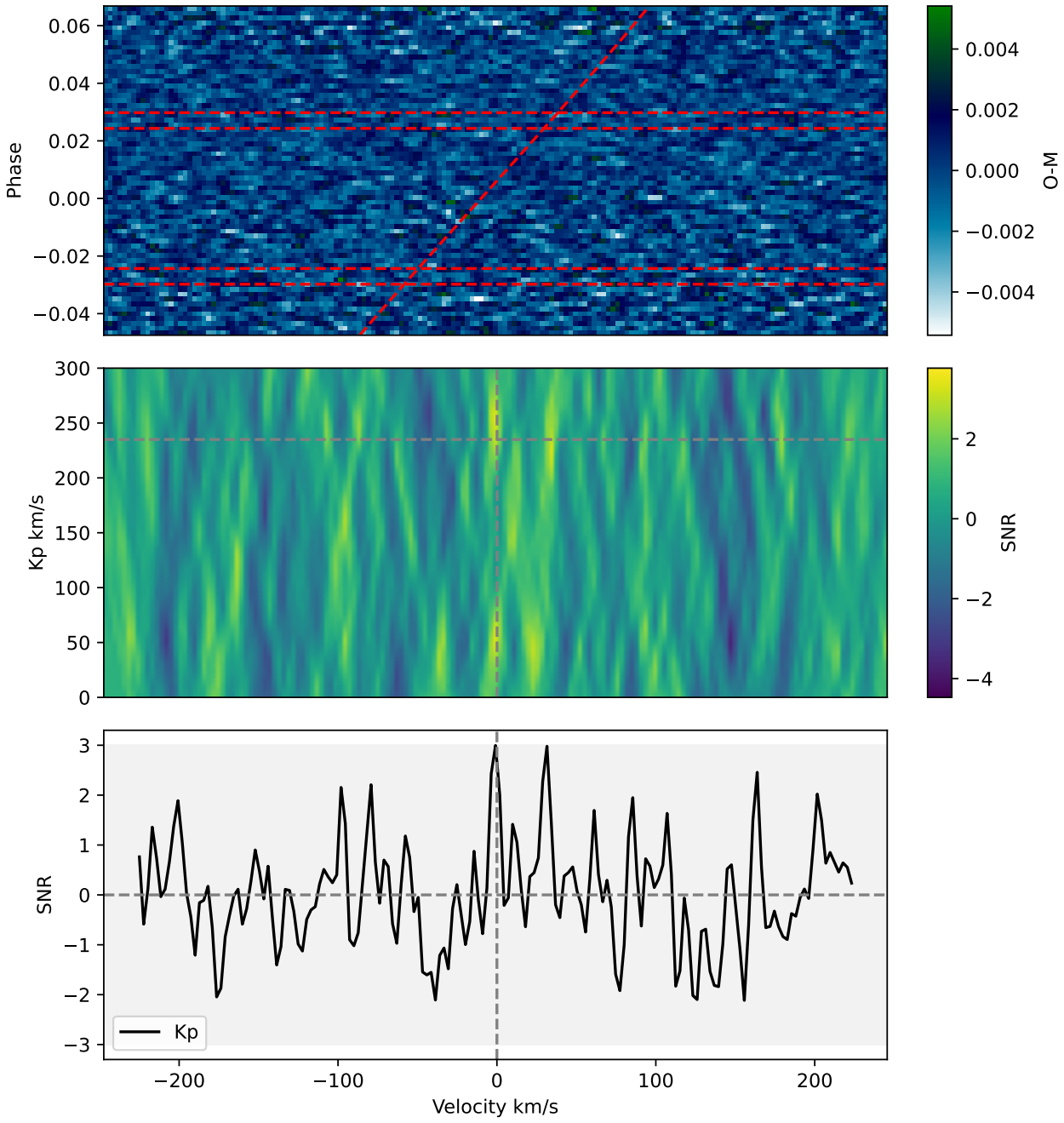

Figure 14: Results of the HAT-P-57 b on 2019-06-28 night analysis showing a possible detection of water. Top) the residual map obtained from the cross-correlation. The tilted dashed red line represents the molecule fingerprint evolution during the observation, and the horizontal dashed red lines represent the different phases of the transit, the first line is T_1 so the next scales to T_2. Middle) the K_P map which shows the distribution of the cross-correlated signal in terms of the semi-amplitude velocity, the systematic velocity and the SNR. The vertical dashed lines are centred in zero due to the reference frame being on the planet and the horizontal line marks the planet's K_P. Bottom) the "slice" of the CCF that belongs to the K_P of the planet. The black line is the signal detected after applying cross-correlation and the grey contour is limited to $\mid 3 \mid \sigma$, which is our initial detection criterion.

For the second night, I had 74 spectral frames distributed as seen in Fig. 15. I used 17 for the analysis. The highest SNR iteration is the 6^{th} one. As a first result, I found a possible detection of CO_2 with a significance of $\sim 4.7\sigma$, Fig. 16. This case is going to be discussed in Sect. 6.

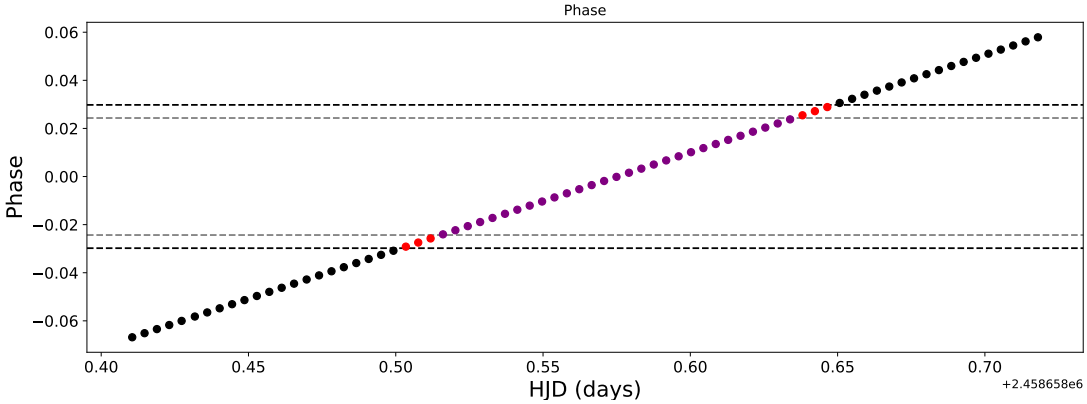

Figure 15: Phase diagram for 2019-06-23 night of HAT-P-57 b.

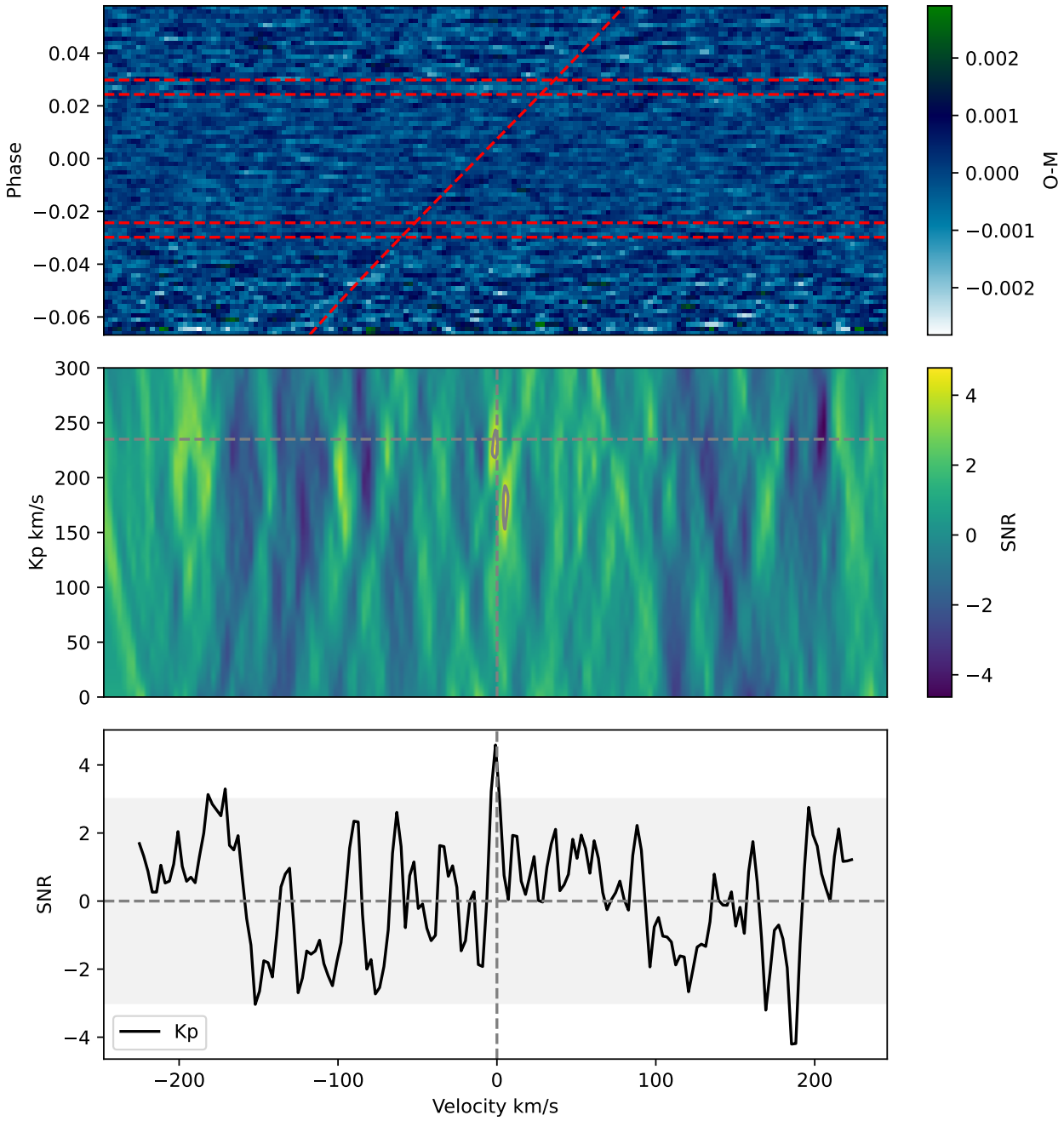

Figure 16: Result of the HAT-P-57 b's 2019-06-23 night analysis showing a possible detection of of CO_2.

5.1.2. KELT-17 b.2019-01-26

For this night, I had 72 spectral frames distributed as seen in Fig. 17. I used 31 orders and the 10^{th} iteration of SYSREM. I detected a clear signal of FeH of $\sim 4.8\sigma$ shown in Fig. 18.

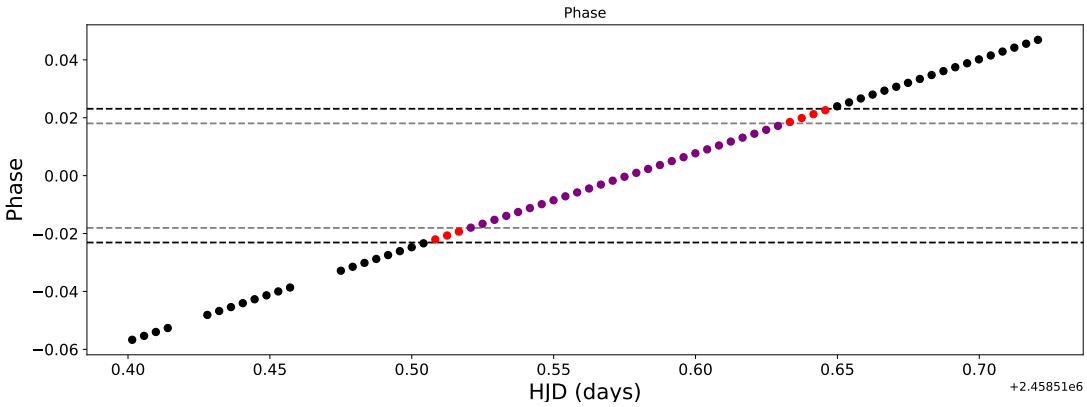

Figure 17: Phase diagram for 2019-01-26 night of KELT-17 b.

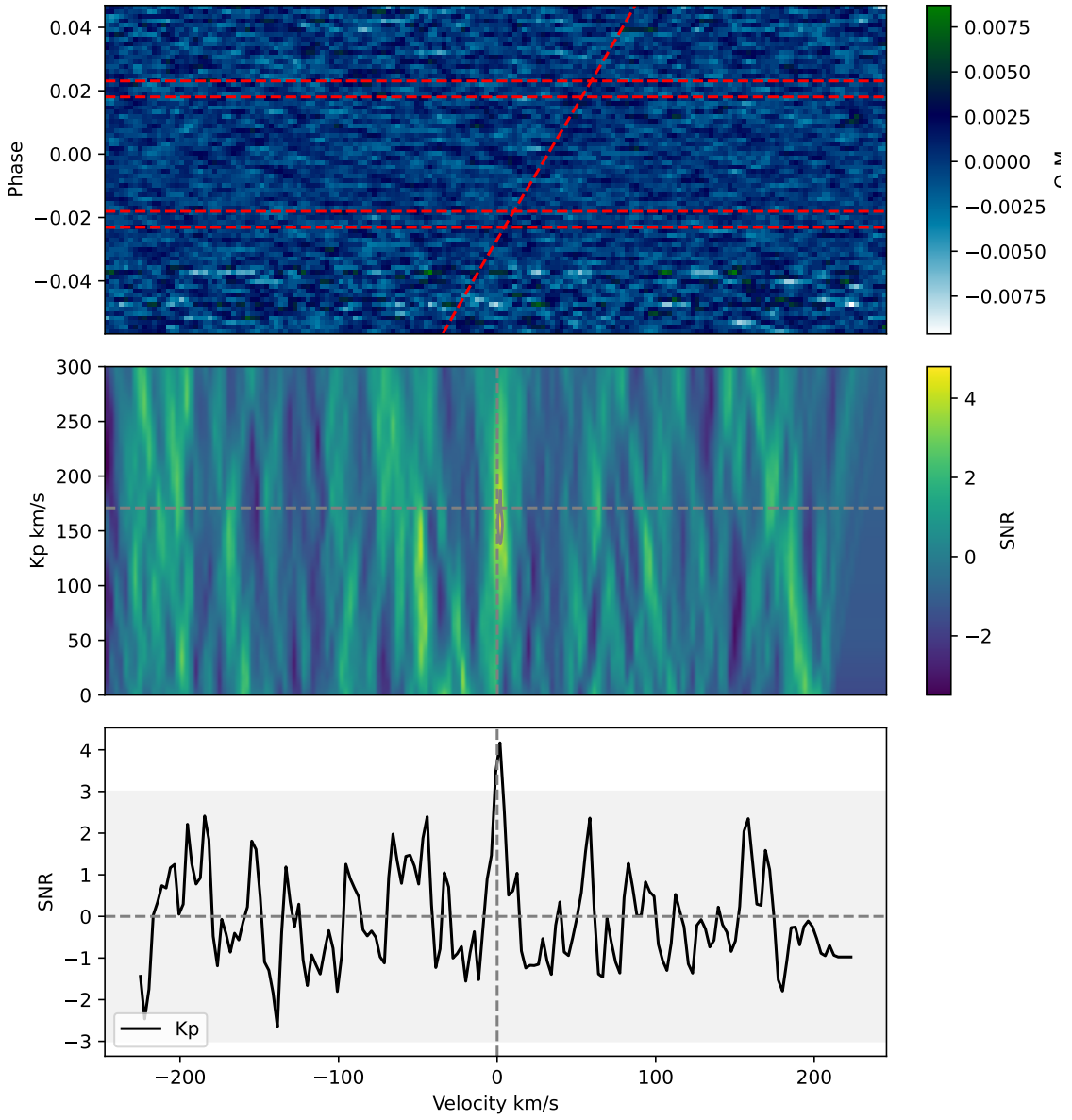

Figure 18: Result of the KELT-17 b's 2019-01-26 night analysis showing a detection of of FeH.

5.2. Non-Detections

5.2.1. KELT-17 b. 2019-01-23

For this night I had 78 spectral frames distributed as seen in Fig. 19. I used 26 orders and the 6^{th} iteration of SYSREM. I did not detect anything for any molecule, Fig. 20. This is the only non-detection image that I am showing to not overload the text with non-detection images which show the same information.

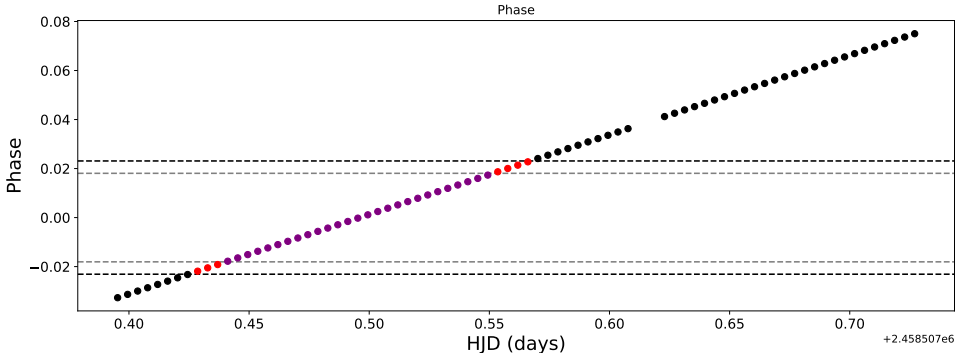

Figure 19: Phase diagram for 2019-01-23 night of KELT-17 b.

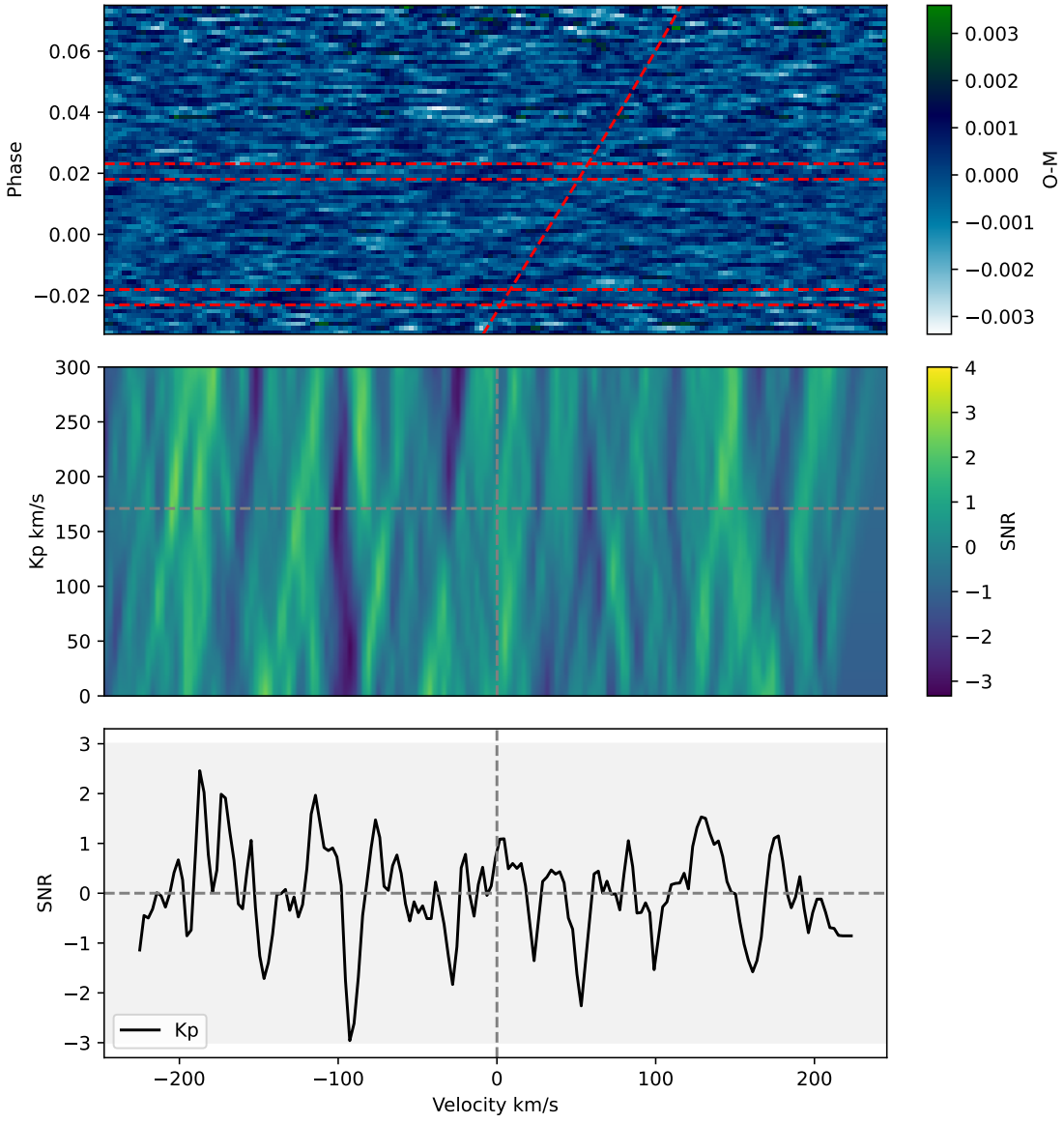

Figure 20: Result of the KELT-17 b's 2019-01-23 night analysis in the case of CO.

5.2.2. KELT-21 b

For this ultra-hot Jupiter, I only had a night, 2019-08-12, with 78 spectral frames with a phase evolution as shown in Fig. 21. I used 16 orders and the 9^{th} iteration of SYSREM. In this case, I did not find anything for any molecule.

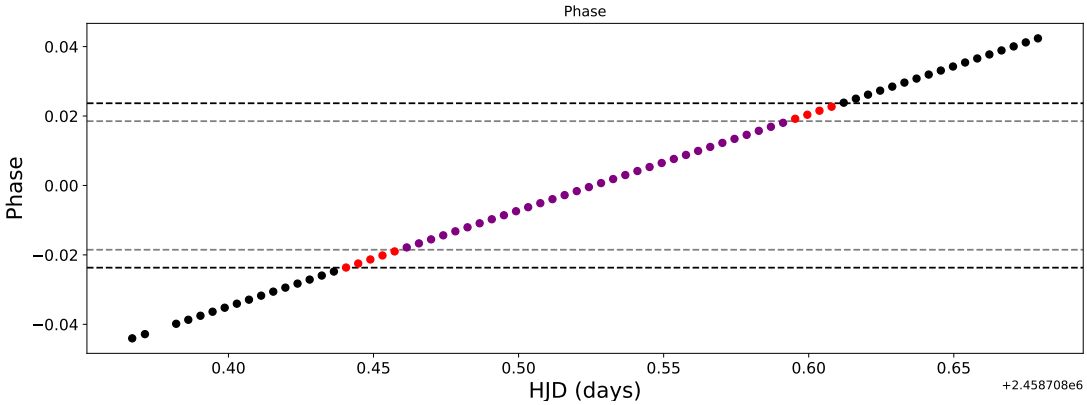

Figure 21: Phase diagram for 2019-08-12 night of KELT-21 b.

5.2.3. WASP-189 b

For this ultra-hot Jupiter, I only had a night, 2019-05-06, with 156 spectral frames with a phase evolution as shown in Fig. 22. I used 24 orders and the 9^{th} iteration of SYSREM. In this case, I did not find anything for any molecule.

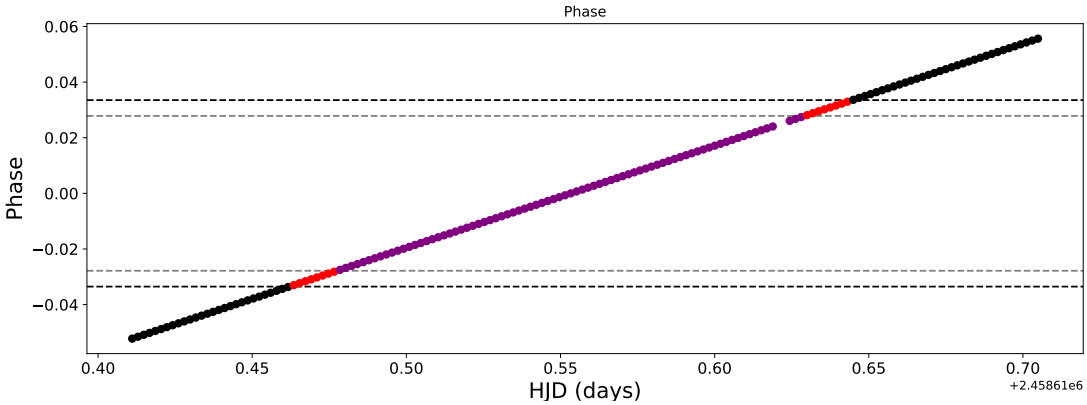

Figure 22: Phase diagram for 2019-05-06 night of WASP-189 b.

5.2.4. HD 189733 b

For this hot Jupiter, I only had a night, 2017-05-30, with 88 spectral frames with a phase evolution as shown in Fig. 23. I used 24 orders and the 9^{th} iteration of SYSREM. In this case, I did not find anything for any molecule.

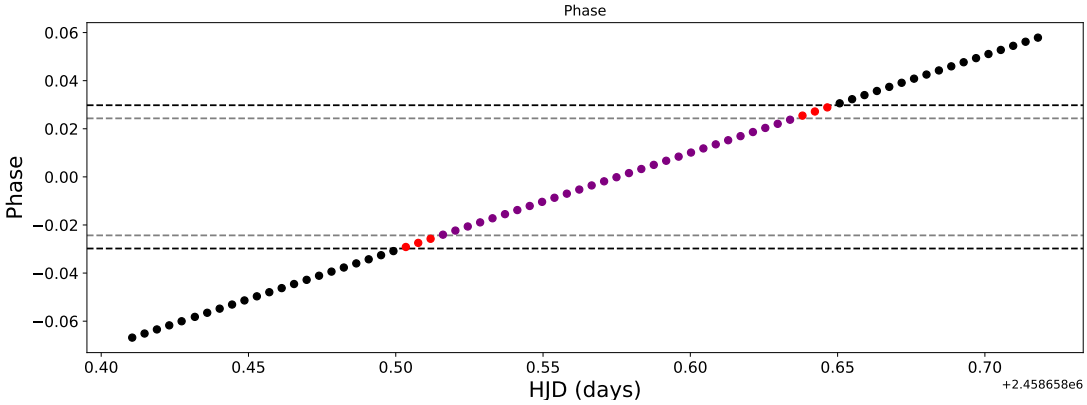

Figure 23: Phase diagram for 2017-05-30 night of HD 189733 b.

6. Discussion

6.1. Detections

In the case of HAT-P-57 b, I found two strange signals. For the night of 2019-06-28, I found a soft signal of water with a significance of $\sim 3.6\sigma$. However, I would not take this as a positive result due to the low significance, I followed the criteria of all the signals being lower than 4.5σ is not considered a detection. Additionally, other signals with similar significance appear in my analysis which could mean a bad data treatment or order selection in this case. If we look at the SNR plot in Fig. 24, the SNR is too low. For my study, I set the criterion that any signal lower than 60 SNR is not high enough to claim the signal detected came from the planet.

Figure 24: Signal-to-noise evolution during the observation on 2019-06-28 night for HAT-P-57 b.

For the 2019-06-23 night for the same planet, I got a clear signal of carbon dioxide of $\sim 4.6\sigma$ as you can see in Fig. 16, but again for this planet, the SNR is so low (Fig. 25) that I cannot be sure about this detection.

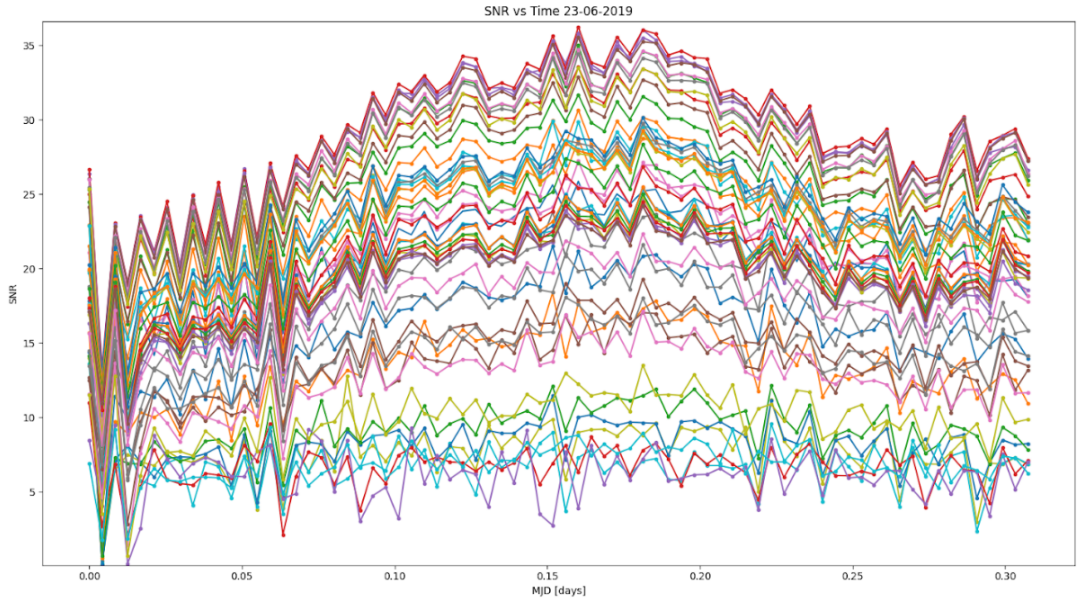

Figure 25: Signal-to-noise evolution during the observation on 2019-06-23 night for HAT-P-57 b.

For this planet, no detections have been released until the moment I am writing this composition, even in Stangret et al. [2021] they did not find anything. Another important problem with this planet is that the uncertainty in the planet's mass causes a large uncertainty in the planet's semi-amplitude velocity, $235 \pm 254\,[\mathrm{km/s}]$, which also makes it challenging to analyse it properly.

Then, I can analyze KELT-17 b, I had two nights but I only had a positive result in 2019-01-26. For the data taken on 2019-01-23, I did not get any result that could be justified by taking a look at the SNR plot, again, in Fig. 26 and noticing the loss of signal occurring in the middle of the transit.

Figure 26: Signal-to-noise evolution during the observation on 2019-01-23 night forKETL-17 b.

For KELT-17 b's second night, 2019-01-26, I had a great detection of iron hydride (FeH) with a significance of $\sim 4.8\sigma$ as can be seen in Fig. 18. Stangret et al. [2021] did not find anything in optical, so I cannot claim that the detection is completely reliable, but, due to the clear signal, I can say

that more observations and studies would be justified to guarantee the existence of FeH in KELT-17 b atmosphere. In this case, the SNR was stable during the night, and no external problems were mentioned during the observation. The next step should be to analyse other available nights for this planet to make a combined detection to improve the quality and reduce the uncertainty of the detection.

6.2. Non-detections

Non-detections are what I expected for most of these planets. Since UHJs and HJs are dominated by metals, as shown in Sect. 1.2 and these are easy to detect in the optical range due to their opacity dominance in that range.

In the case of KELT-21 b, looking at Stangret et al. [2021], they found nothing for this planet, even in the optical range, so the prospect for this planet in the NIR was bad, and I did not find anything there.

Another planet they studied in Stangret et al. [2021] is WASP-189 b, where they found a high-significance signal for Fe I and Fe II, so I expected to find traces of FeH. However, this planet has such a high temperature that all the Fe in its atmosphere is completely dissociated. Other expected molecules were CO detected in Yan et al. [2022] using GIANO-B, too but in that case, they were observing the secondary transit, which means they had the spectra of the planet's dayside, so they had more signal coming from it than me because I studied the primary transit which means all the signal that I received was just from the starlight that went through the planet terminator. While this difference is likely the main reason why I have not detected CO, another possible cause is a strong loss of signal during the observation as seen in Fig. 27 which happened in the middle of the transit.

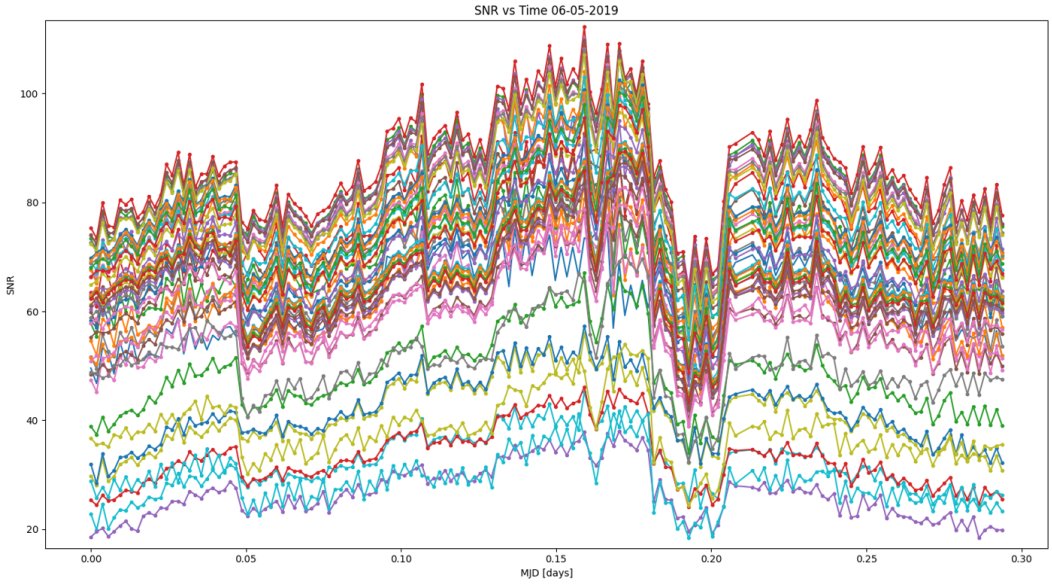

Figure 27: Signal-to-noise evolution during the observation on 2019-05-06 night for WASP-189 b.

The result for HD 189733 b is the expected one due to the data treatment I have done. As mentioned in Brogi et al. [2016] this planet is very affected by strong vertical winds and by the Rossiter-McLaughlin effect, and in this work, we have avoided this kind of data analysis. It is also

important to mention that for this planet there were no problems with the SNR during the night. If we compare my result with Birkby et al. [2013], Cabot et al. [2019], we can see that they detected H_2O on both works and HCN and CO in Dr. Cabot's work, but using dayside spectra which makes sense with the disparities in the result. If I compare my results with Changeat et al. [2022], they found water and CO but they combined observations of the HST G141 grism and the Spitzer Space Telescope, so the comparison with a ground-based telescope is not fair. In other articles like Alonso-Floriano et al. [2019], they observed with CARMENES, Boucher et al. [2021], which use data from SPIRou, Blain et al. [2024], again using CARMENES, and Finnerty et al. [2024], which used Keck data, they obtained positive results for water, CO and carbon dioxide, but I have to mention that the resolution of this instruments is much higher that GIANO-B's one.

7. Conclusions

In this work, I have developed a cross-correlation pipeline GIANO-B, which consists of the data selection and reduction; normalisation; application of SYSREM and the cross-correlation. I also created the atmosphere models and analyse the data searching for some complex molecules in UHJs and HJ.

The main scientific results are the detection of FeH in KELT-17 b, two other possible detections in HAT-P-57 b and the non-detections for the rest of the planets, which was the expected result due to the extreme conditions of UHJs atmospheres introduced in 1.2.

In advance, it would be interesting to continue analysing these planets using other instruments like CRIRES+, with higher resolution, and applying different methods like the single-line method as they do in Casasayas-Barris et al. [2017, 2020] in order to find meaningful lines as helium or magnesium.

Personally, it feels like a victory for me as it was the first time I faced this kind of analysis and I was not only able to reach the goal but to get over it.

Acknowledgement

For those who believed in me. For those who have been my company and my support along this time. I would like to remember you all my family, my girlfriend, Rafael Boix, Hannu, Enric, Jaume, etc. This is for you all.

Especially for my parents who have loved me above all, even when they did not understand what I was doing or why I was doing that. Thank you for trusting me.

As a last mention, I would like to give a shout-out to those who did not believe in me and told me during my bachelor I was not enough for this, a huge hug to them, this is also thanks to you all. Now, I'll continue in Spanish.

Este siempre ha sido mi sueño y estoy aqui gracias a todo el mundo que me ha acompañado nunca voy a olvodarme de esto. Para mí es lo mas importante que me ha pasado y me va a pasar en la vida. Voy a recordar cada momento, cuando me aceptaron en el máster, cuando llegué al despacho de Enric llevando solo una semana y me ofreció observar y me explico como funcionaba todo, la primera reunión con Hannu (y los 300 consiguientes mails), todas las veces que he molestado a Jaume,

quitándole tiempo de su tésis para arreglar mis resultados y, por supuesto, este momento en el que estais leyendo las últimas palabras de un hombre extremadamente afortunado que ha podido cumplir su sueño.

También me gustaría acordarme de la única persona que me hubiera comprendido a la hora de realizar este trabajo, mi tío Manuel de Castro, o Manolo, como lo llamabamos todos. Él era el único doctorado que ha habido en mi familia y era un acérrimo amante de la astronomía y la astrofísica. Siempre me decía que este hubiera sido su sueño, poder vivir de estudiar y observar el universo. Lamentablemente, Manolo murió antes de verme cumplir nuestro sueño, pero a pesar de eso esto también va por él. Estoy seguro de que estaría incluso más orgulloso de mí que yo mismo. Gracias Manolo estés donde estés por ser la única persona de la familia que comprendía y compartía esta pasión conmigo.

Si alguien lee esto y no sabe si dedicarse a la investigación, siempre dicen que ser investigador es duro y probablemente lo sea, pero el camino para llegar ahí lo es aún más, te siente muy solo y necesitas apoyarte en tus compañeros, gracias a Newton, yo he tenido a los mejores. Pero que la soledad no te pare porque si llegas al final y miras atrás, el orgullo que sientes no es comparable a ninguna otra cosa que vayas a sentir o hayas sentido.

Un saludo y muchas gracias por leer.

References

Brett Addison, Duncan J Wright, Robert A Wittenmyer, Jonathan Horner, Matthew W Mengel, Daniel Johns, Connor Marti, Belinda Nicholson, Jack Soutter, Brendan Bowler, et al. Minerva-australis. i. design, commissioning, and first photometric results. *Publications of the Astronomical Society of the Pacific*, 131(1005):115003, 2019.

F Javier Alonso-Floriano, A Sánchez-López, Ignas AG Snellen, Manuel López-Puertas, E Nagel, Pedro J Amado, FF Bauer, JA Caballero, S Czesla, L Nortmann, et al. Multiple water band detections in the carmenes near-infrared transmission spectrum of hd 189733 b. *Astronomy & Astrophysics*, 621:A74, 2019.

Martin Asplund, Nicolas Grevesse, A. Jacques Sauval, and Pat Scott. The Chemical Composition of the Sun. , 47(1):481–522, September 2009. doi: 10.1146/annurev.astro.46.060407.145222.

J. L. Birkby, R. J. De Kok, M. Brogi, E. J. W. De Mooij, H. Schwarz, S. Albrecht, and I. A. G. Snellen. Detection of water absorption in the day side atmosphere of HD 189733 b using ground-based high-resolution spectroscopy at 3.2 Mm. *Monthly Notices of the Royal Astronomical Society: Letters*, 436(1):L35–L39, November 2013. ISSN 1745-3933, 1745-3925. doi: 10.1093/mnrasl/slt107.

J. L. Birkby, R. J. De Kok, M. Brogi, H. Schwarz, and I. A. G. Snellen. Discovery of Water at High Spectral Resolution in the Atmosphere of 51 Peg b. *The Astronomical Journal*, 153(3):138, March 2017. ISSN 0004-6256, 1538-3881. doi: 10.3847/1538-3881/aa5c87.

Doriann Blain, Alejandro Sánchez-López, and Paul Mollière. A formally motivated retrieval framework applied to the high-resolution transmission spectrum of hd 189733 b. *The Astronomical Journal*, 167(4):179, 2024.

Anne Boucher, Antoine Darveau-Bernier, Stefan Pelletier, David Lafrenière, Étienne Artigau, Neil J Cook, Romain Allart, Michael Radica, René Doyon, Björn Benneke, et al. Characterizing exoplanetary atmospheres at high resolution with spirou: detection of water on hd 189733 b. *The Astronomical Journal*, 162(6):233, 2021.

M Brogi, RJ De Kok, S Albrecht, IAG Snellen, JL Birkby, and H Schwarz. Rotation and winds of exoplanet hd 189733 b measured with high-dispersion transmission spectroscopy. *The Astrophysical Journal*, 817(2):106, 2016.

M. Brogi, P. Giacobbe, G. Guilluy, R. J. De Kok, A. Sozzetti, L. Mancini, and A. S. Bonomo. Exoplanet atmospheres with GIANO: I. Water in the transmission spectrum of HD 189 733 b. *Astronomy & Astrophysics*, 615:A16, July 2018. ISSN 0004-6361, 1432-0746. doi: 10.1051/0004-6361/201732189. URL https://www.aanda.org/10.1051/0004-6361/201732189.

AGA Brown, Antonella Vallenari, TJDBJH Prusti, JHJ De Bruijne, C Babusiaux, CAL Bailer-Jones, M Biermann, Dafydd Wyn Evans, Laurent Eyer, Femke Jansen, et al. Gaia data release 2-summary of the contents and survey properties. *Astronomy & astrophysics*, 616:A1, 2018.

Timothy M. Brown. Transmission Spectra as Diagnostics of Extrasolar Giant Planet Atmospheres. *The Astrophysical Journal*, 553(2):1006–1026, June 2001a. ISSN 0004-637X. doi: 10.1086/320950.

Timothy M Brown. Transmission spectra as diagnostics of extrasolar giant planet atmospheres. *The Astrophysical Journal*, 553(2):1006, 2001b.

Samuel HC Cabot, Nikku Madhusudhan, George A Hawker, and Siddharth Gandhi. On the robustness of analysis techniques for molecular detections using high-resolution exoplanet spectroscopy. *Monthly Notices of the Royal Astronomical Society*, 482(4):4422–4436, 2019.

N. Casasayas-Barris, E. Palle, G. Nowak, F. Yan, L. Nortmann, and F. Murgas. Detection of sodium in the atmosphere of WASP-69b. *Astronomy & Astrophysics*, 608:A135, December 2017. ISSN 0004-6361. doi: 10.1051/0004-6361/201731956.

N. Casasayas-Barris, E. Pallé, F. Yan, G. Chen, S. Kohl, M. Stangret, H. Parviainen, Ch. Helling, N. Watanabe, S. Czesla, A. Fukui, P. Montañés-Rodríguez, E. Nagel, N. Narita, L. Nortmann, G. Nowak, J. H. M. M. Schmitt, and M. R. Zapatero Osorio. Atmospheric characterization of the ultra-hot Jupiter MASCARA-2b/KELT-20b. *Astronomy & Astrophysics*, 640:C6, August 2020. ISSN 0004-6361. doi: 10.1051/0004-6361/201935623e.

Quentin Changeat, Billy Edwards, Ahmed F Al-Refaie, Angelos Tsiaras, Jack W Skinner, James YK Cho, Kai H Yip, Lara Anisman, Masahiro Ikoma, Michelle F Bieger, et al. Five key exoplanet questions answered via the analysis of 25 hot-jupiter atmospheres in eclipse. *The Astrophysical Journal Supplement Series*, 260(1):3, 2022.

David Charbonneau, Timothy M Brown, Robert W Noyes, and Ronald L Gilliland. Detection of an Extrasolar Planet Atmosphere. *ApJ*, 568(1):377–384, March 2002. ISSN 0004-637X. doi: 10.1086/338770.

A Collier Cameron, Don Pollacco, RA Street, TA Lister, Richard G West, DM Wilson, F Pont, DJ Christian, WI Clarkson, B Enoch, et al. A fast hybrid algorithm for exoplanetary transit searches. *Monthly Notices of the Royal Astronomical Society*, 373(2):799–810, 2006.

M Cropper, D Katz, P Sartoretti, T Prusti, JHJ De Bruijne, F Chassat, P Charvet, J Boyadjian, M Perryman, G Sarri, et al. Gaia data release 2-gaia radial velocity spectrometer. *Astronomy & Astrophysics*, 616:A5, 2018.

Rebekah I. Dawson and John Asher Johnson. Origins of Hot Jupiters. *Annual Review of Astronomy and Astrophysics*, 56(1):175–221, September 2018. ISSN 0066-4146, 1545-4282. doi: 10.1146/annurev-astro-081817-051853. URL https://www.annualreviews.org/doi/10.1146/annurev-astro-081817-051853.

Luke Finnerty, Jerry W Xuan, Yinzi Xin, Joshua Liberman, Tobias Schofield, Michael P Fitzgerald, Shubh Agrawal, Ashley Baker, Randall Bartos, Geoffrey A Blake, et al. Atmospheric metallicity and c/o of hd 189733 b from high-resolution spectroscopy. *The Astronomical Journal*, 167(1):43, 2024.

Jonathan J Fortney, Rebekah I Dawson, and Thaddeus D Komacek. Hot jupiters: origins, structure, atmospheres. *Journal of Geophysical Research: Planets*, 126(3):e2020JE006629, 2021.

Joel D Hartman, GÁ Bakos, Lars A Buchhave, G Torres, David W Latham, Géza Kovács, W Bhatti, Zoltan Csubry, Miguel de Val-Borro, K Penev, et al. Hat-p-57b: A short-period giant planet transiting a bright rapidly rotating a8v star confirmed via doppler tomography. *The Astronomical Journal*, 150 (6):197, 2015.

Ekaterina S Ivshina and Joshua N Winn. Tess transit timing of hundreds of hot jupiters. *The Astrophysical Journal Supplement Series*, 259(2):62, 2022.

C Jiang, G Chen, E Pallé, F Murgas, H Parviainen, and Y Ma. Featureless transmission spectra of 12 giant exoplanets observed by gtc/osiris. *Astronomy & Astrophysics*, 675:A62, 2023.

Marshall C Johnson, Joseph E Rodriguez, George Zhou, Erica J Gonzales, Phillip A Cargile, Justin R Crepp, Kaloyan Penev, Keivan G Stassun, B Scott Gaudi, Knicole D Colón, et al. Kelt-21b: A hot jupiter transiting the rapidly rotating metal-poor late-a primary of a likely hierarchical triple system. *The Astronomical Journal*, 155(2):100, 2018.

D Katz, P Sartoretti, Mark Cropper, P Panuzzo, GM Seabroke, Y Viala, K Benson, R Blomme, Gérard Jasniewicz, A Jean-Antoine, et al. Gaia data release 2-properties and validation of the radial velocities. *Astronomy & Astrophysics*, 622:A205, 2019.

A Kokori, A Tsiaras, B Edwards, A Jones, G Pantelidou, G Tinetti, L Bewersdorff, A Iliadou, Y Jongen, G Lekkas, et al. Exoclock project. iii. 450 new exoplanet ephemerides from ground and space observations. *The Astrophysical Journal Supplement Series*, 265(1):4, 2023.

M Lendl, Sz Csizmadia, A Deline, L Fossati, Daniel Kitzmann, Kevin Heng, S Hoyer, Sébastien Salmon, Willy Benz, Chris Broeg, et al. The hot dayside and asymmetric transit of wasp-189 b seen by cheops. *Astronomy & Astrophysics*, 643:A94, 2020.

Michel Mayor and Didier Queloz. A Jupiter-mass companion to a solar-type star. *Nature*, 378 (6555):355–359, November 1995. ISSN 0028-0836, 1476-4687. doi: 10.1038/378355a0. URL https://www.nature.com/articles/Art1.

P. Mollière, J. P. Wardenier, R. van Boekel, Th. Henning, K. Molaverdikhani, and I. A. G. Snellen. petitradtrans: A python radiative transfer package for exoplanet characterization and retrieval. *Astronomy amp; Astrophysics*, 627:A67, July 2019. ISSN 1432-0746. doi: 10.1051/0004-6361/201935470. URL http://dx.doi.org/10.1051/0004-6361/201935470.

E. Oliva, L. Origlia, R. Maiolino, C. Baffa, V. Biliotti, P. Bruno, G. Falcini, V. Gavriousev, F. Ghinassi, E. Giani, M. Gonzalez, F. Leone, M. Lodi, F. Massi, I. Mochi, P. Montegriffo, M. Pedani, E. Rossetti, S. Scuderi, M. Sozzi, and A. Tozzi. The GIANO spectrometer: towards its first light at the TNG. page 84463T, Amsterdam, Netherlands, October 2012. doi: 10.1117/12.925274. URL http://proceedings.spiedigitallibrary.org/proceeding.aspx?doi=10.1117/12.925274.

Leonardo A Paredes, Todd J Henry, Samuel N Quinn, Douglas R Gies, Rodrigo Hinojosa-Goñi, Hodari-Sadiki James, Wei-Chun Jao, and Russel J White. The solar neighborhood xlviii: nine giant planets orbiting nearby k dwarfs, and the chiron spectrograph's radial velocity performance. *The Astronomical Journal*, 162(5):176, 2021.

Timo Prusti, JHJ De Bruijne, Anthony GA Brown, Antonella Vallenari, C Babusiaux, CAL Bailer-Jones, U Bastian, M Biermann, Dafydd Wyn Evans, L Eyer, et al. The gaia mission. *Astronomy & astrophysics*, 595:A1, 2016.

Roman R. Rafikov. Can Giant Planets Form by Direct Gravitational Instability? *The Astrophysical Journal*, 621(1):L69–L72, March 2005. ISSN 0004-637X, 1538-4357. doi: 10.1086/428899. URL https://iopscience.iop.org/article/10.1086/428899.

Roman R. Rafikov. Atmospheres of Protoplanetary Cores: Critical Mass for Nucleated Instability. *The Astrophysical Journal*, 648(1):666–682, September 2006. ISSN 0004-637X, 1538-4357. doi: 10.1086/505695. URL https://iopscience.iop.org/article/10.1086/505695.

Monica Rainer, Avet Harutyunyan, Ilaria Carleo, Ernesto Oliva, Serena Benatti, Andrea Bignamini, Riccardo Claudi, Esther Gonzalez-Alvarez, Nicoletta Sanna, Adriano Ghedina, Giuseppina Micela, Emilio Molinari, Andrea Tozzi, Carlo Baffa, Andrea Baruffolo, Nicolas Buchschacher, Massimo Cecconi, Rosario Cosentino, Gilberto Falcini, Daniela Fantinel, Luca Fini, Alberto Galli, Francesca Ghinassi, Elisabetta Giani, Carlos Gonzalez, Manuel Gonzalez, Raffaele Gratton, Jose Guerra, Marcos Hernandez Diaz, Nauzet Hernandez, Marcella Iuzzolino, Marcello Lodi, Luca Malavolta, Jesus Maldonado, Livia Origlia, Hector Perez Ventura, Alfio Puglisi, Carlos Riverol, Luis Riverol, Jose San Juan, Salvo Scuderi, Ulf Seeman, Alessandro Sozzetti, and Mauro Sozzi. Introducing GOFIO: a DRS for the GIANO-B near-infrared spectrograph. In *Ground-based and Airborne Instrumentation for Astronomy VII*, volume 10702, pages 1855–1864. SPIE, July 2018. doi: 10.1117/12.2312130. URL https://www.spiedigitallibrary.org/conference-proceedings-of-spie/10702/1070266/Introducing-GOFIO--a-DRS-for-the-GIANO-B-near/10.1117/12.2312130.full.

Lee J Rosenthal, Benjamin J Fulton, Lea A Hirsch, Howard T Isaacson, Andrew W Howard, Cayla M Dedrick, Ilya A Sherstyuk, Sarah C Blunt, Erik A Petigura, Heather A Knutson, et al. The california legacy survey. i. a catalog of 178 planets from precision radial velocity monitoring of 719 nearby stars over three decades. *The Astrophysical Journal Supplement Series*, 255(1):8, 2021.

S. Seager and D. D. Sasselov. Theoretical Transmission Spectra during Extrasolar Giant Planet Transits. *The Astrophysical Journal*, 537(2):916–921, July 2000. ISSN 0004-637X. doi: 10.1086/309088.

Ignas A. G. Snellen, Remco J. de Kok, Ernst J. W. de Mooij, and Simon Albrecht. The orbital motion, absolute mass and high-altitude winds of exoplanet HD 209458b. *Nature*, 465(7301):1049–51, June 2010. ISSN 1476-4687. doi: 10.1038/nature09111.

M. Stangret, N. Casasayas-Barris, E. Pallé, F. Yan, A. Sánchez-López, and M. López-Puertas. Detection of Fe I and Fe II in the atmosphere of MASCARA-2b using **a** cross-correlation method. *Astronomy & Astrophysics*, 638:A26, June 2020. ISSN 0004-6361, 1432-0746. doi: 10.1051/0004-6361/202037541.

M. Stangret, E. Pallé, N. Casasayas-Barris, M. Oshagh, A. Bello-Arufe, R. Luque, V. Nascimbeni, F. Yan, J. Orell-Miquel, D. Sicilia, L. Malavolta, B. C. Addison, L. A. Buchhave, A. S. Bonomo, F. Borsa, S. H. C. Cabot, M. Cecconi, D. A. Fischer, A. Harutyunyan, J. M. Mendonça, G. Nowak, H. Parviainen, A. Sozzetti, and R. Tronsgaard. The obliquity and atmosphere of the ultra-hot Jupiter TOI-1431b (MASCARA-5b): A misaligned orbit and no signs of atomic ormolecular absorptions. *Astronomy & Astrophysics*, 654:A73, October 2021. ISSN 0004-6361, 1432-0746. doi: 10.1051/0004-6361/202040100.

M. Stangret, N. Casasayas-Barris, E. Pallé, J. Orell-Miquel, G. Morello, R. Luque, G. Nowak, and F. Yan. High-resolution transmission spectroscopy study of ultra-hot Jupiters HAT-P-57b, KELT-17b, KELT-21b, KELT-7b, MASCARA-1b, and WASP-189b. *Astronomy & Astrophysics*, 662:A101, June 2022. ISSN 0004-6361, 1432-0746. doi: 10.1051/0004-6361/202141799.

Keivan G Stassun, Karen A Collins, and B Scott Gaudi. Accurate empirical radii and masses of planets and their host stars with gaia parallaxes. *The Astronomical Journal*, 153(3):136, 2017.

Otto Struve. Proposal for a project of high-precision stellar radial velocity work. *The Observatory, Vol. 72, p. 199-200 (1952)*, 72:199–200, 1952.

O. Tamuz, T. Mazeh, and S. Zucker. Correcting systematic effects in a large set of photometric light curves. *Monthly Notices of the Royal Astronomical Society*, 356(4):1466–1470, February 2005. ISSN 00358711, 13652966. doi: 10.1111/j.1365-2966.2004.08585.x. URL https://academic.oup.com/mnras/article-lookup/doi/10.1111/j.1365-2966.2004.08585.x.

F Yan, E Pallé, A Reiners, N Casasayas-Barris, D Cont, M Stangret, L Nortmann, P Mollière, Th Henning, G Chen, et al. Detection of co emission lines in the dayside atmospheres of wasp-33b and wasp-189b with giano. *Astronomy & Astrophysics*, 661:L6, 2022.

George Zhou, Joseph E Rodriguez, Karen A Collins, Thomas Beatty, Thomas Oberst, Tyler M Heintz, Keivan G Stassun, David W Latham, Rudolf B Kuhn, Allyson Bieryla, et al. Kelt-17b: A hot-jupiter transiting an a-star in a misaligned orbit detected with doppler tomography. *The Astronomical Journal*, 152(5):136, 2016.